Automated Detection and Counting of Pedestrians and Bicyclists Along an Urban Roadway

**U.S. Department of Transportation
Federal Highway Administration**

massDOT
Moving Massachusetts Forward
Massachusetts Department of Transportation

Deval L. Patrick	**Timothy P. Murray**	**Richard A. Davey**
Governor	*Lieutenant Governor*	*Secretary & CEO*

Technical Report Document Page

1. Report No. SPRII.03.25	2. Government Accession No. n/a	3. Recipient's Catalog No. n/a
4. Title and Subtitle Automated Detection and Counting of Pedestrians and Bicyclists Along an Urban Roadway		5. Report Date June 30, 2012
		6. Performing Organization Code
7. Author(s) Russell Tessier, Daiheng Ni		8. Performing Organization Report No. UMTC-XX
9. Performing Organization Name and Address 309G Knowles Engineering Building, University of Massachusetts, Amherst, MA 01003		10. Work Unit No. (TRAIS) n/a
		11. Contract or Grant No. 59641
12. Sponsoring Agency Name and Address Massachusetts Department of Transportation Office of Transportation Planning Ten Park Plaza, Suite 4150, Boston, MA 02116		13. Type of Report and Period Covered Final Report June 2012
		14. Sponsoring Agency Code n/a
15. Supplementary Notes n/a		

16. Abstract

As urban transportation planning becomes more sophisticated, the accurate detection and counting of pedestrians and bicyclists becomes more important. In this project, two distinct camera-based approaches are integrated together to create a real-time pedestrian and bicyclist counting system which is regularly accurate to 85% and often achieves higher accuracy. The primary approach retasks a state-of-the-art traffic camera, the Autoscope Solo Terra, for pedestrian and bicyclist counting. Object detection regions are sized to identify multiple pedestrians moving in either direction on an urban sidewalk and bicyclists in an adjacent bicycle lane. Collected results are processed in real time, eliminating the need for video storage and postprocessing. Although this primary approach shows high accuracy, in some cases undercounting or overcounting of pedestrians can occur. To combat these issues, a second camera can be used to identify pedestrian heads and shoulders. Image recognition is then used to improve the accuracy of the count while still allowing the overall combined approach to operate in real time. In this report, results are presented for a pedestrian walkway for pedestrian flow up to 108 persons/min and the limitations of the implemented system are enumerated.

17. Key Word Bicyclist counting, pedestrian counting, urban roadway, automated counting, camera, counting algorithms		18. Distribution Statement unrestricted	
19. Security Classif. (of this report) unclassified	20. Security Classif. (of this page) unclassified	21. No. of Pages	22. Price

Form DOT F 1700.7 (8-72)   Reproduction of completed page authorized

AUTOMATED DETECTION AND COUNTING OF PEDESTRIANS AND BICYCLISTS ALONG AN URBAN ROADWAY

Final Report

Prepared By:

Russell Tessier
Principal Investigator

Daiheng Ni
Co-Principal Investigator

309G Knowles Engineering Building
University of Massachusetts
Amherst, MA 01003

June 2012

Acknowledgements

Disclaimer

v

Executive Summary

This study of Automated Detection and Counting of Pedestrians and Bicyclists Along an Urban Roadway was undertaken as part of the Massachusetts Department of Transportation (MassDOT) Research Program. This program is funded with Federal Highway Administration (FHWA) Statewide Planning and Research (SPR) funds. Through this program, applied research is conducted on topics of importance to the Commonwealth of Massachusetts transportation agencies.

As accommodations for pedestrians and bicyclists become an increasingly important part of urban transportation planning, there is a growing need for accurate counts of these groups. Pedestrian and bicyclist count data can be used for a variety of purposes, including intersection planning, bicycle lane allocation, sidewalk design, and traffic light deployment, among others. It has been shown that pedestrian and bicyclist injuries and deaths in urban areas can be significantly reduced by the use of effective transportation infrastructure. Accurate pedestrian and bicyclist counting methodologies serve as important resources for urban planners by providing accurate data that can assist transportation planning.

The counting of pedestrians and bicyclists has been an active research topic for over ten years. To be useful, pedestrian and bicyclist counting systems must meet a series of criteria. A system must be accurate, easy to deploy, and cost effective. Current standards indicate a need for at least 85% count accuracy over a time period of hours for count data to be used effectively in transportation planning. The use of human assistants to collect counts in real time is not only labor intensive, but it can be highly inaccurate. Early efforts to automate counting with low complexity equipment, such as pressure sensors, have met with limited success due to their inaccuracy. However, recent improvements in digital camera and imaging software technology have made advances in bicyclist and pedestrian counting more feasible. Most recent imaging-based counting systems require the storage and post processing of image data to achieve accurate counts, a significant individual privacy concern. Also, many current camera-based counting systems are quite complex and require significant user expertise for proper operation.

In an effort to address the limitations of previous pedestrian and bicyclist counting systems, an advanced camera-based system has been developed for this project. The new system retasks an existing traffic camera, the Autoscope Solo Terra, which typically is used to detect and count motor vehicles at intersections and on highways to focus on pedestrian and bicyclist counting. For the project, a series of software enhancements have been made to the equipment to optimize the detection of pedestrians and bicyclists both on a sidewalk and in an adjacent roadway bicycle lane. All counts are determined in real time, using software embedded within the camera and additional software algorithms implemented in an attached personal computer. The key algorithm used to identify pedestrians considers the size of an object located in an image zone in comparison with the known size of a pedestrian object. Bicyclists are located by the presence of an object in a specific image zone for a period of time. To increase accuracy, a second camera can be used to collect additional images which can be used to verify pedestrian counts from the first camera. The second camera uses a pedestrian recognition technique based on the identification of a pedestrian's head and shoulders. Multiple identifications in an image frame indicate the presence of multiple pedestrians. The use of a second camera is not needed for bicyclist detection since the single-camera approach is sufficiently accurate.

The software interface for the developed system is easy to use. A transportation employee can easily deploy the system by assembling the system with simple tools and clicking on several icons on a personal computer desktop. For advanced use, software can be adjusted to become more or less sensitive to individual pedestrians and bicyclists. Our testing has indicated that high count accuracy can be achieved for a range of settings. Two deployment platforms have been constructed and tested for the camera-based system. An initial platform based on a stepladder was used to generate the results documented in this report. In the latter stages of the project, the stepladder was replaced by a trailer which can easily be attached to a transportation department motor vehicle. This ruggedized system is available for immediate deployment by transportation department employees in areas where pedestrian and bicyclist counts are needed. In both cases, the retasked traffic camera is mounted on an extendable pole and pointed perpendicular to the flow of pedestrian and bicyclist traffic.

To verify the results of the system, a series of experiments were performed at the University of Massachusetts and in downtown Boston. Pedestrian traffic on an enclosed footbridge, an open pedestrian path, and an urban sidewalk were evaluated over a span of more than ten minutes per experiment. Through experimentation it was found that our system can successfully detect and count pedestrians moving in a single direction on a sidewalk with over 85% accuracy. The approach also successfully counts pedestrians moving in opposite directions on the same sidewalk at the same rate. Bicyclist counting with accuracy similar to pedestrian counting is limited to unidirectional flow for bicyclists operating in a lane adjacent to an urban sidewalk. The accuracy of our approach is limited by a sensitivity to shadows and strong bursts of sunshine. Future enhancements in imaging software may help address these issues.

In conclusion, this effort to build a practical, easy-to-use, and accurate pedestrian and bicyclist counting system has resulted in a deployable system which is highly accurate. The system has been tested on an urban roadside for an extended period of time to determine its long-term effectiveness. Future work will involve making the system more robust to solar glare, shadows, and darkness. Further testing in a variety of weather conditions would also be desirable. As a result of this work, it is recommended that a pilot project be established that allows for the extensive collection of bicyclist and pedestrian data in a variety of real world urban roadway environments. Given the immediate need for this data and the availability of the functional prototype, the collection of this data can have significant short and long term benefits for urban transportation planning.

Table of Contents

List of Tables

List of Figures

1.0 Introduction

This study of Automated Detection and Counting of Pedestrians and Bicyclists Along an Urban Roadway was undertaken as part of the Massachusetts Department of Transportation (MassDOT) Research Program. This program is funded with Federal Highway Administration (FHWA) Statewide Planning and Research (SPR) funds. Through this program, applied research is conducted on topics of importance to the Commonwealth of Massachusetts transportation agencies.

As urban transportation planning becomes more sophisticated, the accurate detection and counting of bicyclists and pedestrians becomes more important. Accurate counts can be used to determine the need for additional pedestrian walkways and intersection reorganization, among other planning initiatives. In this project, two distinct camera-based approaches are integrated together to create a real-time pedestrian and bicyclist counting system which is regularly accurate to 85% and often achieves higher accuracy. The primary approach retasks a state-of-the-art traffic camera, the Autoscope Solo Terra, for pedestrian and bicyclist counting. Object detection zones are resized to identify multiple pedestrians moving in either direction on an urban sidewalk. Bicyclists in a bicycle lane adjacent to the sidewalk are counted separately. Collected results are processed in real time, eliminating the need for video storage and postprocessing. Although this primary approach shows high accuracy, in some cases due to occlusion, undercounting or overcounting of pedestrians can occur. To combat these issues, a second camera can be used to identify pedestrian heads and shoulders. Image recognition is then used to improve the accuracy of the count while still allowing the overall combined approach to operate in real time. In this report, results are presented for a pedestrian walkway for a variety of pedestrian traffic densities and the limitations of the implemented system are enumerated.

1.1 Objectives

Every year pedestrian fatalities constitute around 12 percent of all traffic fatalities causing approximately 4,000 deaths and 59,000 injuries (*1*). The fatalities are more frequent in urban areas than in rural areas due to the higher volume of pedestrians. For the safe accommodation of pedestrian and bicyclist traffic, transportation planning requires an accurate estimate of the occupancy of walkways and bicycle lanes (*2*)(*3*) and their effects on urban pedestrian and traffic accidents (*4*). This information can be particularly useful in prioritizing pedestrian-oriented projects (*5*), forecasting future pedestrian demand (*5*), and evaluating the need for automated traffic control systems (*6*). Hiring human resources to count pedestrians at various locations at different times of the day over a long period is a cost-ineffective solution. The need to explore automated techniques that detect and count pedestrians allows for the economical collection of data pertaining to pedestrian traffic which is required for transportation planning process. Such data may be used to alert drivers to pedestrians in the vicinity of vehicles, enhancing safety.

A solution for pedestrian and bicyclist counting must consider a number of factors. The system must be automated to allow for the efficient, economical and accurate collection of pedestrian and bicyclist traffic data. An automated counting system can be deployed on a wide scale only if the

system provides counts with an accuracy of at least 85%. The system must be able to operate in real time without the need for video storage or postprocessing. The system must operate for a variety of pedestrian flow densities and in a variety of environmental conditions. Each of these issues is addressed in this research.

Overall, the specific objectives of this research project were:

- To make necessary software and hardware adjustments to a commercial traffic camera-based system to perform the required detection and counting of pedestrians and bicyclists on and adjacent to an urban sidewalk.
- To integrate the camera-based system into a portable platform that can be rapidly deployed in an urban environment.
- To develop plans to deploy copies of the system more widely.

This research addresses the challenge of acquiring the data needed to achieve these goals and objectives in an efficient and cost effective way and is supportive of existing pedestrian and bicyclist programs at all levels.

1.2 System Overview

Our system addresses issues in pedestrian and bicyclist counting by integrating two image processing-based technologies in a new and complementary fashion. An available traffic camera, which is primarily designed and used for the detection and counting of motor vehicles, is retasked to identify pedestrians and bicyclists. For pedestrian counting, this technology primarily works using a series of small detection zones which are triggered by one or more pedestrians. Pedestrians cover multiple zones for a fixed period of time leading to accurate counts. In some cases, due to occlusion or lighting, exact pedestrian counts can vary from actual pedestrian traffic. Our system integrates a second, image processing based approach which relies on a histogram of gradients (HoG) algorithm (7) to identify a pedestrian's head and shoulders. The instantaneous count identified by the HoG approach is compared against the count determined by the zone-based approach for validation. Bicyclist counting uses similar zone-based approaches.

A series of experiments have been performed using the integrated experimental setup at the University of Massachusetts, Amherst and in downtown Boston. Pedestrian traffic on an enclosed footbridge, an open pedestrian path, and an urban sidewalk were evaluated over a span of more than ten minutes per experiment. Real time pedestrian counts taken using the zone-based method alone exhibited better than 85% accuracy while the combined detection zone/HoG approach consistently approached 90% accuracy. Tests were performed for a variety of pedestrian foot-traffic densities. Similar accuracy was determined for bicyclist counting.

1.3 Report Outline

The remainder of this report is structured in the following fashion. In Section 2, the details of the traffic camera-based system and its integrated components are discussed. The section also describes extensions which allowed for the integration of the image-processing based approach. Section 3 presents experimental results and a discussion of current system limitations. Section 4 provides recommendations for the future deployment of the system and examines next steps. Section 5 concludes the report and summarizes our work.

2.0 Research Methodology

In this chapter we describe our pedestrian and bicyclist counting system in addition to providing appropriate background. The details of our experimental setup are also provided.

2.1 Background and Related Work

A variety of techniques have previously been used to detect and count pedestrians and bicyclists in a selection of scenarios (bicycle paths, intersections, sidewalks, etc). The approaches have typically used infrared beam sensors, laser scanners, pressure sensors, and image-based approaches, among others. Passive infrared radar beam sensors (*8*)(*9*) have been used to detect and classify motor vehicles for over ten years (*10*). A typical sensor projects two infrared beams across the width of a traffic lane. These sensors generate grey scale images based on the heat emitted by the human body. The intensity of a pixel corresponds to the temperature of the target object. Although the approach is robust for a variety of lighting conditions, it can be inaccurate due to the error rate caused by heat emitted from clothing worn by pedestrians. Furthermore, the system does not efficiently detect still pedestrians. In general, the technology associated with infrared sensors has not progressed much in recent years. The enclosures used to hold the beam-generating lasers are somewhat bulky and most data transfer from these units is made via slow serial connections. It also appears that beam widths may not be sufficiently wide to detect a range of pedestrian movements.

Laser scanners (*11*) provide an alternative approach. Laser pulses, which are switched on for a very short duration, illuminate a scene. A camera lens gathers the reflected light and projects it onto a sensor plane for object identification. The nature and extent of the reflections are used to differentiate pedestrians and other objects. These systems have a tendency to consume a lot of energy (*11*) and are generally not used for crowded pedestrian environments. Complex signal processing operations are also often required which can lead to inaccurate counts. An alternative technology, pressure sensors, has been found to be effective (*12*) for counting in some cases, although sensors must be deployed in the direct path of pedestrian traffic. This approach is considered to be somewhat outdated for significant pedestrian traffic flows (*6*). Ultrasonic heat detection sensors have recently been used to address the pedestrian and bicyclist detection and counting problem. These units use reflected ultrasonic waves to detect the body heat of pedestrians and bicyclists within a relatively short range. Although relatively straightforward to configure and use, ultrasonic systems are limited in terms of their application space. These sensors are generally most appropriate for low traffic volume areas where pedestrians and bicyclists pass by infrequently and do not obstruct one another.

Most state-of-the-art pedestrian counters use compute-intensive image processing techniques to classify and count pedestrians. Computer vision based techniques employ images or videos obtained from a lens-based camera to single out objects that are likely to be pedestrians. The simplest approach to extract information about pedestrian candidates is through background subtraction, the process of removing background information from an image. Objects extracted from the resulting foreground are passed as inputs to a classification stage. In general, an object is identified as a pedestrian by comparing a sub-image to a library of previously-stored sub-images. The likelihood of

a match against an image template is determined via statistical means using approaches such as support vector machines (SVM) (*7*) and the histogram of gradients (HoG) approach (*7*). Once an object is identified as one or more pedestrian candidates, it is counted. The object is then tracked until it leaves the camera window so it is not counted a second time. In many cases, the observed area is wide (*3*)(*6*) (e.g. a town square) and sparsely populated. The lack of pedestrian occlusion assists the image recognition problem by limiting the number of required object evaluations. More complicated image processing approaches attempt to break "blobs" of pedestrians in zones into individual counts (*4*)(*13*). Iterative processing is sometimes performed on the blobs (4)(14) to more accurately determine pedestrian count. In general, these approaches require a lengthy training time for each evaluated location (*4*)(*13*)(*14*) which sometimes exceeds the recording time. Almost all reported cases operate on recorded video (*4*)(*6*)(*14*), although in some cases it appears they could work in real time without the use of recorded video. A previous image processing based approach which does not require recorded video (*3*) evaluates a pedestrian walkway with low pedestrian density which is tens of meters in width. A summary of previously-applied approaches and their general qualities appears in Table 2.1.

Most bicyclist counting projects appear to use manual approaches for counting (*15*), although one project (*16*), which uses an inductive loop, has been reported. This approach is summarized in Table 2.1. In general, bicyclist counting on an urban roadway is easier to perform than pedestrian counting since bicyclists can be assumed to travel in a single direction in a bicycle lane at the edge of the roadway while pedestrians travel in the same or opposing directions on an adjacent sidewalk.

Table 2.1: Summary of different pedestrian and bicyclist counting techniques

Technique	Candidate Generation	Advantages	Disadvantages
Infrared sensor	Heat generated by human body	• Established technology • Robust against lighting changes	• Dependence on clothing • Limited coverage area • Inability to detect still pedestrians
Laser Scanner	Time-of-flight	• Covers multiple pedestrians • Easy setup	• Computationally complex • Not robust against weather.
Ultrasonic sensor	Heat generated by human body	• Easy to use	• Perform poorly with crowds
Histogram of Oriented Gradient	Computer Vision	• High accuracy	• Difficulty to detect pedestrians in various poses
Zone based detection	Computer Vision	• Sufficient accuracy • Large coverage area	• Only pedestrians parallel to image plane detected • Hardware limitations
Inductive Loop	Magnetism	• Accuracy	• Difficult to deploy

In general, these previously-used techniques have drawbacks which make them challenging to use in an urban environment. In this work, our primary approach uses a modern traffic camera to identify pedestrians and bicyclists and counts them as they pass through fixed image zones.

2.2 Basic System Implementation

The primary system used for our experimentation includes a traffic camera mounted on a custom-made pedestal. For this initial approach, video processing techniques typically used for vehicle detection are applied to pedestrian and bicyclist detection and counting. The camera used for experimentation is the Autoscope Solo Terra (*17*) from Econolite, Inc. The field of view of the camera is split into multiple detection zones that are defined by a user. The Solo Terra was selected after examining cameras from competitors Iteris, Inc. and Traficon at the start of the project in late 2009. At the time of the evaluation, none of the camera products from these companies included the ability to transfer data in real time from detection zones to an attached personal computer for further processing.

For the Solo Terra, when an object (e.g. a pedestrian or bicyclist) passes through the zone, a detection event is triggered and the object can be counted. In normal operation, the Solo Terra uses these zones to detect the presence of vehicles. In our application, pedestrians on and bicyclists adjacent to a sidewalk are detected and counted. A complete system including a Solo Terra camera, a custom pedestal, and an attached personal computer is used to detect and count pedestrians. A custom suite of software has been written to analyze data from the camera in real time. The entire system has been tested in the field for a wide range of traffic flows. Its robust operation is demonstrated for periods of up to ten minutes.

Figure 2.1: The Solo Terra camera based system. The camera is located on the left and the interface panel is in the middle.

2.2.1 Autoscope Solo Terra Traffic Camera

The Autoscope Solo Terra includes a high resolution camera (PAL/CCIR: 752 x 582 pixels, NTSC/RS170: 768 x 494 pixels) and two processing chips, a TI DaVinci TMS320DM6446 dual core

digital signal processor and an ARM926 microprocessor core. The camera is capable of collecting snapshots of the field of view and calculating and storing traffic statistics without human intervention. The TMS320CC64x+ core performs image processing operations over the image frame. General purpose processing for control and data transfer is handled by the ARM926 core (*17*). Data from the camera is periodically downloaded to an attached personal computer (PC) through the three-phase power cable to an interface panel at intervals ranging from once per second to once per several days. The interface panel transmits the collected data to the PC through a standard Ethernet cable, as shown in Figure 2.1. The panel provides power to the camera and protects it from transient current surges in addition to providing power to the camera unit.

The Solo Terra has a number of built-in software features which can be used for vehicle detection and counting. The software embedded within the camera can be used to allow users to select multiple image regions of different sizes in the camera field of view. Such detector regions, or zones, are constantly monitored for any activity. The Autoscope software provides different types of regions, including presence detector regions, count detector regions, and others depending on the monitoring purpose. The number of Solo Terra detector regions is limited to 99, which provides more than sufficient coverage for most applications. As shown in Figure 2.2, count detectors, which span a lane of traffic, can be designated by a user. Each time a motor vehicle passes through the count detector, the count is increased by one. Two consecutive motor vehicles in the same lane can be differentiated by the gap between the vehicles. The count is accumulated over a specific time period to generate a total. If one detector is allocated per lane, the count over an entire highway can be identified.

Figure 2.2: Solo Terra count detectors (yellow lines) allocated to lanes of a highway.
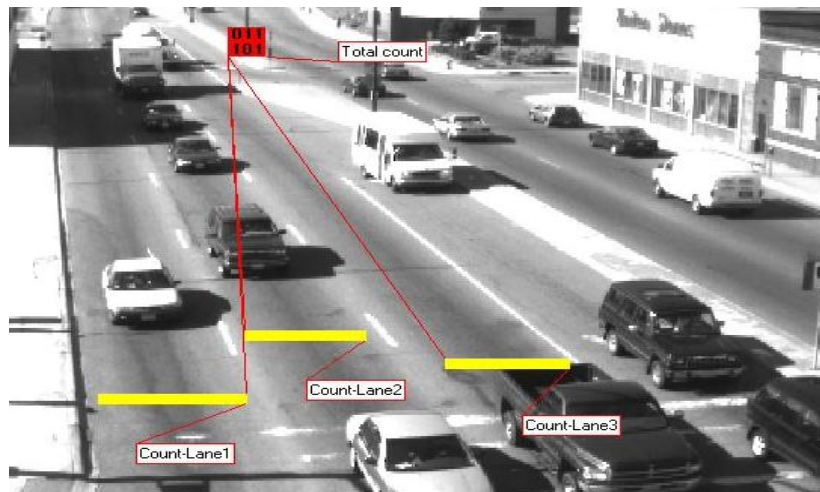
The direct use of this type of approach for pedestrian counting presents some obvious problems.

- Pedestrians are much smaller in size than motor vehicles and represent a smaller portion of an overall image.
- Pedestrians walking on a sidewalk generally do not stay in fixed lanes or move in a single direction.
- Many pedestrians may be present in an image frame at a given point in time.

As a result, Autoscope Solo Terra count detectors cannot be directly applied to the pedestrian and counting problem. In the following subsections we describe new ways to use *presence* detector regions in an Autoscope Solo Terra image using configuration software that comes with the Solo Terra. Presence data from these regions are then transferred to the attached PC and processed to identify pedestrians and bicyclists at specific points in time. Counts are then derived from this presence information. All count processing is performed in real time on the PC attached to the Solo Terra setup.

2.2.2 Description of Approach

Our pedestrian counting system consists of a Solo Terra camera, the interface panel and a PC with the counting software running on it (similar to Figure 2.1). The Solo Terra camera is mounted on a custom-made pedestal with provisions to adjust the mounting height and angle. Extension cords connect the interface panel to power outlets near the test locations. Presence detector regions in the camera field of view are selected for monitoring pedestrian movements.

Figure 2.3: Initial support structure for Solo Terra pedestrian and bicyclist counting system

The hardware support structure for the Solo Terra (Figure 2.3) was built at the Mechanical Engineering Workshop at the University of Massachusetts, Amherst. The design objectives were low cost, portability, ready availability of raw materials, and robustness against weather and uneven surfaces. The structure has provisions to adjust the mounting height and angle of the camera to carry out experiments. The maximum height supported by the structure is 15 feet. The support structure employs an eight foot stepladder as a stable base for mounting the camera. The lightweight ladder is collapsible and easy to transport. A drilled hole on the top of the ladder accommodates a pipe which acts as the main mounting pole. This main pipe is fixed to the ladder with the help of angle iron and C-shaped clamps. Short, sharpened reinforcing bars (rebars) on the bottom end of

the main pipe penetrate into the ground thus fixing the position of the structure. Four additional pieces of rebar may be added for further support by means of C-shape clamps. The position of the rebars on the ladder can be adjusted to ensure penetration into uneven ground and reduce slight movements due to windy weather.

A smaller pipe inserted into the top end of the main pipe facilitates the adjustment of the mounting height. The length of the inner pipe can be varied from 2 ft to 4 ft. Hence, the total length of the mounting pole ranges between the 12 ft and 14 ft span that satisfies the system requirements. A flange was installed on the top of the pipe to connect to the adjustable camera bracket. If the length of the rebars and the camera bracket is taken into account, the maximum mounting height is 15 ft.

The structure provides access to the adjustable pipe as well as the camera to fine-tune the height and angle of tilt by allowing an operator to climb up the ladder. The angle of tilt can be varied using a wrench. The camera can be manually swiveled and inclined by the adjustable bracket attached to it. The hardware support system requires a straightforward installation procedure. All individual parts can be assembled to build the final structure in the field in twenty minutes. An insulated enclosure is provided for the interface panel to ensure safe operation. The box is placed beside the step ladder. A long power cable connects the interface panel to a power source.

Presence detectors in the Autoscope Solo Terra system operate by identifying changes in the portion of the image covered by the detector. This change is identified by pixel color, lightness, and contrast differences from a previously-stored background. When the camera is first turned on, the system operator selects the position and size of detectors using vendor-supplied configuration software running on the PC. As shown in Figure 2.4, detectors can be quite small.

Figure 2.4: Two columns of uniformly distributed presence detectors

Initially, when a detector is not covered by a pedestrian or vehicle, it has an "off" status. Video streamed from the camera to the PC shows these "off" detectors in black. When a pixel in the

9

detector is covered by a pedestrian its status changes to "on". This change is noted by a green color in the detectors in Figure 2.4. Note the use of many small detectors in Figure 2.4. If the detector size is enlarged to match the size of an entire pedestrian, the number of pedestrians may frequently be overcounted since a single pedestrian may walk through multiple adjacent zones. In field tests it was observed that the amount of overcount can be a factor of two or more, although the overcount amount was not consistent. This issue can be addressed through the use of multiple vertical columns of small detectors, as shown in Figure 2.4. In this configuration there are two columns of small size presence detectors which are uniformly distributed in the columns. Because distances between adjacent presence detectors are relatively small, every person passing through the columns of detectors triggers substantially more than one presence detector. As will be shown in Chapter 3, in general, the number of detectors a single person can trigger can roughly be considered a constant. The on/off status of presence detectors is updated very rapidly by the Solo Terra (on the order of fractions of a second), so gaps between consecutive pedestrians can be noted.

In our approach, presence detector on/off information is downloaded from the Autoscope Solo Terra to the attached PC every second as a plain text file. An example of the transferred information is shown in Figure 2.5. Detector status information is only transmitted when a detector's status transitions from "on" to "off" or "off" to "on". These status changes represent a pedestrian passing through a sidewalk region which includes the detector. The arrival of a pedestrian is represented as an "off"-to-"on" and the departure of a pedestrian is represented as "on"-to-"off". An "on"-to-"off" transition is represented by a logical 0 and an "off"-to-"on" state is represented by a logical 1. The text file in Figure 2.5 contains information such as the detector number, date, time, ticks and state. Column entries for date, detector number, time and state are self-explanatory. Every row contains information for a single detector transition. The column labeled "ticks" identifies changes in milliseconds. All detector transitions are recorded by the Solo Terra as soon as they happen although the transition file is only transferred from the Solo Terra to the PC once per second.

Figure 2.5: Example of polled data information from the Autoscope camera

```
detector;     date    ;     time   ; ticks ;state
  number
     110;3/25/2011;11:58:47 AM;1470216;0;
     112;3/25/2011;11:58:47 AM;1470316;0;
     111;3/25/2011;11:58:47 AM;1470383;0;
     112;3/25/2011;11:58:49 AM;1473119;1;
     112;3/25/2011;11:58:50 AM;1473453;0;
     112;3/25/2011;11:58:51 AM;1474754;1;
     112;3/25/2011;11:58:51 AM;1474888;0;
     118;3/25/2011;11:58:52 AM;1475789;1;
     117;3/25/2011;11:58:52 AM;1475855;1;
     118;3/25/2011;11:58:52 AM;1475956;0;
     117;3/25/2011;11:58:52 AM;1476022;0;
```

Three pedestrian counting approaches were developed based on this retrieved presence information. In the next three subsections, we discuss *state averaging*, *state matrix*, and *threshold* approaches.

2.2.3 State Averaging Approach

In this approach, two columns of detectors are placed on the image (e.g. inside the red box in Figure 2.6). The Solo Terra only reports transitions in the detector states. The number of OFF-ON transitions in one second for a column are counted and divided by a constant. The time and position coordinates of the affected detectors are not considered, although during experiments it was observed that vertically adjacent detectors are most likely to have the same ON state. While dividing, decimal values are rounded off. It can be noted that pedestrians that are closer to the camera (e.g. at the bottom of the picture in Figure 2.6) occupy less area than pedestrians farther from the camera.

Hence, we tried experiments with a uniform spacing of detectors and a non-uniform spacing of detectors. Surprisingly, the uniform spacing and gradient spacing approach generated about equal results in terms of accuracy. All of the following approaches allow for detection of up to three pedestrians traversing presence detector zones at the same time. The pedestrians can be traveling in the same or in opposite directions.

Figure 2.6: Detector configuration used in the state averaging approach

2.2.4 State Matrix Approach

The time and position of the detectors is taken into account in the state matrix approach. One column of detectors is used (Figure 2.7) and, like the state averaging approach, changes in presence detector states are noted. Unlike the state averaging approach, the position of the detectors in the column undergoing an OFF-ON-OFF change is also considered in performing counting. The position of the farthest and the closest detector to the camera which undergo changes are used to approximate the general area of movement. The amount of vertical space (e.g. number of detectors aligned vertically) occupied by a pedestrian for a specific camera mounting height is used to determine the number of pedestrians. Depending on how many detectors undergo changes, the pedestrian count is increased by 1, 2 or 3.

Figure 2.7: Detector configuration used for the state matrix approach

This approach addresses the scenarios where an insufficient number of detectors do not turn ON for the averaging approach. Since the algorithm depends on the number of consecutive vertical detectors which exhibit OFF-ON-OFF behavior, the error is high if the detectors at the top or bottom of a sequence of vertically-aligned detectors do not act as expected. In our experimentation, the average count accuracy of the approach was about 40%, primarily due to undercounting. As a result, further experimentation with the approach was abandoned in favor of the state averaging approach which considers the total number of detector transitions in multiple columns irrespective of where the detectors are located.

2.2.5 Threshold Approach

The threshold approach considers that a pedestrian covers a constant number of detectors (M) out of consecutive group of N vertical detectors. As shown in Figure 2.8 inside the red box, a single column of presence detectors is configured. The column can be divided into overlapping groups, each consisting of N detectors. The count is incremented when at least M detectors belonging to a group of N turn ON simultaneously. The amount of the count increment depends on the number of groups which satisfy the ON condition. Two detector configurations were tried for this approach. One consisted of a column of 13 detectors, with each detector set to a size of 2 x 9 pixels. The second configuration consisted of a column of 15 detectors, each of size 9 x 2 pixels. A feature in the Solo Terra camera software which can detect the triggering of M out of N detectors was used to determine when count increments should occur.

Figure 2.8: Configuration of 13 detectors for the threshold approach

2.2.6 Limitations of the Presence Detector Approaches

Although Solo Terra presence detectors have been used successfully for this application, a number of limitations did become apparent during experimentation:

- A homogeneous background is best for presence detection. The presence of large cracks or tree branches can negatively impact the count due to false triggering of presence detectors.
- Strong bursts of sunlight can cause the detectors to fail. A shaded area or an area with consistent sunlight is best for detection.
- It is difficult to accurately detect more than three pedestrians at a time given the limits on consecutive detector zones that can be configured across a sidewalk.

Overall, these limitations did not greatly impact our ability to achieve accurate pedestrian counts.

2.2.7 Bicyclist Detection Algorithm Using the Solo Terra

As mentioned in Section 2.1, the detection and counting problem for bicyclists is somewhat easier to address than for pedestrians since bicyclists are assumed to travel in a single direction in a predefined bicycle lane. This configuration differs from the two-way traffic on a sidewalk commonly exhibited by pedestrians.

Figure 2.9: Detector configuration for bicyclist detection

To address this difference, the Solo Terra camera was used in a slightly different way to detect bicyclists versus pedestrians. To detect bicyclists, a speed detector was used. In this case, it is assumed that bicyclists will travel in a single direction in a lane which adjacent to a sidewalk, as shown in Figure 2.9. Speed detectors, when configured for use with the Solo Terra, measure the speed and length of the vehicle passing through it.

The Solo Terra speed detectors are unidirectional, i.e. they are triggered only when the movement is in one particular direction, making them appropriate for our bicyclist detection needs. The speed detectors are trapezoidal in shape with one end (the exit point) wider than the other (the entry

point). Due to this unidirectional property, multiple detectors with opposite orientations could be set up to capture movement in both directions, although this test was not performed in our experimentation. For the configuration shown in Figure 2.9, the detector captures the speed and length information of bicyclists moving from left to right. In our approach, length is used as the parameter for the detection and counting of bicyclists. If the recorded length is about 6 to 8 feet, the vehicle is classified as a bicyclist and the count is increased.

Figure 2.10: Solo Terra system mounted on a portable trailer

2.2.8 Robust Mounting Platform for the Solo Terra

In preparation for delivery of the system to the MassDOT, the camera-based system shown in Figure 2.3 was remounted on a portable trailer and an instruction manual regarding the assembly, configuration, and disassembly of the system was prepared. As seen in Figure 2.10, the system contains several plastic boxes which hold a ruggedized laptop and the Solo Terra interface panel. The laptop which was selected for the platform is a Dell Latitude E6400 XFR. The laptop can be removed from the box on the left in the figure when the camera system is in transport. The Solo Terra is mounted on a retractable 40' fiberglass mast manufactured by Pin Point Technologies. Although not seen in the figure, a solar panel is located on the top of the arrow board. Current from

the panel can be used to charge the battery located in the locked yellow enclosure at the bottom of the trailer. All power for the camera and laptop originates from the battery. An inverter is used to convert voltage from the battery from 12V DC to 120V AC.

The ruggedized assembled system was tested and the pedestrian and bicyclist counting algorithms described in this report were found to work accurately. However, all numerical results included in the report were obtained using the ladder-based structure shown in Figure 2.3.

2.3 Vision Based Shape Detection

In our experimentation, the detection zone approaches described in the previous section form the primary approach used for pedestrian and bicyclist detection in this work. In some cases, however, it is desirable to consider a second approach to be used in conjunction with the primary approach. The goal in this second approach is not stand-alone pedestrian counting. Rather, the technique has been developed to validate counts in the camera image at certain points in time. The approach can be considered complementary to the more accurate and comprehensive approaches described in the previous section. Unlike the previously-described zone-based approaches, our secondary technique attempts to detect a pedestrian's head and shoulders in an image. The count estimates obtained with this approach are then used for comparison with the counts obtained using the zone-based approaches. In the last portion of this section we describe how this image-processing based approach is integrated with the zone-based approach to perform this checking.

2.3.1 Image Processing Overview

In our image-processing approach, image frames without pedestrians are collected from a camera and temporarily buffered. The background of the image is then defined and stored. Subsequently, as pedestrians walk through the image window, the background is subtracted from the obtained images to identify objects that are, potentially, pedestrians. This action is followed by a classification step that identifies the objects as pedestrians or as non-pedestrians. A count of the pedestrians in a frame at a specific time instant can be compared against the count obtained using the traffic camera techniques described in Section 2.2.

The classification of shapes into pedestrian and non-pedestrian categories is carried out by scanning the frame for a distinctive omega "Ω" shape formed by the head and shoulders of a pedestrian (*18*) whenever pixel values are distinguished from the background. Shapes are represented by means of a histogram of oriented gradients (HoG) (*7*). The decision making algorithm is implemented in software as a support vector machine (SVM) (*19*). The output of the SVM is 1 if the algorithm recognizes an "Ω" shape and 0 otherwise. Each positive SVM determination represents a pedestrian detection. An overview of each of the above steps is now presented in subsequent subsections.

2.3.2 Background Determination and Subtraction

Background subtraction identifies whether new objects have entered a frame that is being processed. The previously-determined background is subtracted from a frame to identify new objects and the difference is scaled to reduce the effects of slight pixel brightness variations. Hence, the performance of background subtraction is affected by the pre-determined background as well as the

contrast of foreground objects against the background. In our approach, the background is determined iteratively by converting buffered frames to grayscale images and finding the median values of pixels at each location (*20*). The background can be determined by using the median of each pixel across 10 and 100 frames.

2.3.3 Classification into Pedestrians and Non-Pedestrians

Classification is carried out if the background subtraction process identifies a new object in the current frame. The most critical aspect of classifying objects into pedestrians and non-pedestrians is the selection and representation of a feature that is unique to pedestrians. In our adopted methodology, the "Ω" shape (*21*) formed by the head and shoulders of a human being is used as the feature that distinguishes pedestrians from non-pedestrians. The "Ω" shape approach has been implemented for the following reasons

- The "Ω" shape remains more or less the same regardless of clothing styles.
- The shape is robust against shape variation as a person walks. This characteristic is in contrast to full-body shape recognition where shapes can change dramatically.

The frames containing the new object form the input to the omega shape detector software. Shape detectors rely on a numerical shape representation known as a descriptor vector. The number of elements in the descriptor vector is referred to as the dimension of the descriptor. In the adopted methodology, shapes are represented by HoG descriptors (*7*). The detector calculates descriptors in a given frame and identifies whether they belong to an omega shape. The location of a window containing the "Ω" shape forms the detector output. HoGs provide an excellent description for discriminating objects in the presence of cluttered backgrounds under different illuminations (*7*). The shape of an object can be characterized using a histogram of shape edges, which are pixel locations which have sharp, abrupt changes in brightness values. The calculation of an HoG descriptor requires an image to be divided into dense overlapping windows of a pre-determined size. Each image window is further divided into small regions called cells. The HoG descriptor is calculated for each cell. The edge orientations of all pixels of a cell are allocated to bins where each bin represents a cell characteristic. A collection of bins forms a histogram.

A support vector machine (SVM) is used to classify a histogram as a pedestrian or non-pedestrian. The SVM maps all training samples to a mathematical formula (*19*). If the result of the formula meets an expected value for a pedestrian, a positive result is returned. Otherwise, a negative result is returned. The classification process is assisted by the use of training data where the presence of pedestrians is clearly marked. Effectively, the classifier "learns" which metrics indicate a pedestrian is present so they can be used to locate pedestrians in frames where the presence of pedestrians is unknown.

2.3.4 Data Set and Libraries Used for Training

The set of images used in training directly affects the performance of a classifier. A variety of training images are available, although the INRIA person dataset (*22*) was determined to be the best match. This dataset includes numerous pedestrian images for accurate classification, making it the most desirable choice. The INRIA dataset consists of 614 annotated positive samples containing pedestrians from various locations and 1218 negative samples consisting of roads, landscapes and buildings. The pedestrians are mostly standing, but some images appear in other orientations

portrayed against a wide variety of background images including crowds. The detection algorithms for HoG and SVM were implemented in C++ using OpenCV (*23*) as a main framework component. The OpenCV library is a computer vision library that includes basic computer vision algorithms and machine learning functions.

2.3.5 Integrated System for Accurate Counting

The two counting approaches described in Section 2.2 and Sections 2.3.1-2.3.3 can be viewed as complementary. The omega detection algorithm performs poorly in situations where the head and shoulders of pedestrians are not clearly visible. The Solo Terra approach is more feasible for wide-scale deployment, but there are situations where approximating multiple detectors to the presence of one pedestrian may not work well. Pedestrians farther away from the camera tend to be missed when the sidewalk is fully occupied along its width. None of the Solo Terra counting algorithms effectively address issues such as overcounts and missed counts. As mentioned in Section 2.2, the Solo Terra increments the pedestrian count based on OFF-ON transitions of presence detectors. The detectors turn ON whenever pixel values in detector regions differ from background pixels. At times, shadows of trees and overhead wires may turn the detectors ON resulting in false counts. Overcounts may also occur when certain pedestrians cover more detector regions than an average-sized pedestrian. Such overcounts are generally minimal in the omega detection approach. In some cases, increased lighting (e.g. a burst of sunshine) can lead to camera blooming, as shown in Figure 2.11. This effect can lead to Solo Terra undercounts.

Figure 2.11: Detectors remaining ON due to blooming resulting in undercounts

Since the Solo Terra increments the pedestrian count based on changes in pixel values, an approach is needed that validates the count as it is determined.

2.3.6 Experimental Setup for the Integrated System

The integrated system consists of a Solo Terra camera and a low-cost camera which communicate with a single PC. The PC collects state transition data from the Solo Terra and images from the low cost camera. The two cameras use separate mounting structures to capture videos without disrupting pedestrian traffic. A standard personal camera which can collect video is used in conjunction with the Solo Terra to collect images for HoG processing. In general, images from the same camera

cannot be used for both types of processing since the Solo Terra must be positioned perpendicular to the traffic flow to implement the detection zone approach described in Section 2.2 and a more parallel/planar view is needed for HoG processing.

A single piece of software written in C++ implements the state averaging algorithm described in Section 2.2.3 and the omega detection algorithm described in Chapter 2.3.3 on the PC attached to the cameras. The linear support vector machine (SVM) available in the OpenCV library is used for classification. A count is calculated using detector information obtained from Solo Terra with occasional corrections using the omega detection algorithm. The software monitors the polled state transition data collected by Solo Terra and carries out omega detection under the following conditions. Note that parameter *m* in the following discussion indicates the number of detectors needed to detect a pedestrian using the state averaging approach (Section 2.2.3)

- CASE 1: Whenever more than $n = 1.5 * m$ detectors are ON simultaneously - A snapshot of the field of view is obtained from the low-cost camera. Regions farther from the Solo Terra are scanned for omega shapes. The states of detector regions closer to the Solo Terra at that particular instant are considered for the state averaging approach. The final count at that instant is the sum of counts obtained from both approaches.

- CASE 2 : Whenever more than $n = 1.5 * m$ detectors are ON simultaneously for more than four seconds – This condition indicates that the Solo Terra is refocusing itself. The count is solely incremented based on the omega detection approach until the detectors turn off.

In all other cases, the count is incremented based on the state averaging approach. The count at each instant along with a timestamp is dumped into a text file which can be processed at a later point of time for statistics collection. Overcounts due to shadows of moving branches may be avoided if sufficient detectors are triggered to start the omega detection process. Data from the two cameras are synchronized to allow for correct analysis.

3.0 Results

This chapter details experiments that were conducted for the Solo Terra pedestrian and bicyclist counting approaches described in Section 2.2. Experiments performed for the combined Solo Terra/HoG approach described in Section 2.3.5 are also described. Results for all experiments are presented.

3.1 Pedestrian Counting Setup

Site selection was an important aspect of our experimentation. Site suitability was determined by the presence of an AC power outlet near the location, reasonable pedestrian traffic and walkway widths similar to a sidewalk. Most experiments were conducted under sunny weather conditions with limited shadows and lighting variation. Initial experiments were conducted at two locations on the University of Massachusetts, Amherst campus, a sidewalk adjacent to the Engineering Lab II building and on the Marcus Hall pedestrian ramp (Figure 3.1). Both locations are straight walkways of approximately 8 feet in width, the typical width of a sidewalk. Pedestrian flow rates in these areas were generally measured to be between 5 and 15 persons/min, although flow rates as high as 100 persons/min were measured during peak periods. The dense pedestrian traffic in opposite directions emulated a crowded pedestrian sidewalk in an urban area. The Solo Terra camera was placed near the walkways on the mounting structure described in Section 2.2. The height of the camera was fixed at 15 feet. Results obtained with this setup were later verified during similar experiments using a sidewalk and bicycle lane outside the Massachusetts Transportation Building in Boston, MA.

Figure 3.1: Test locations for counting pedestrians using the Solo Terra (Left: Sidewalk adjacent to the Engineering Lab II building, Right: Marcus Hall pedestrian ramp)

A total of 19 experiments were performed to evaluate the configuration of presence detectors and algorithms. The effectiveness of the system is measured in terms of accuracy and overall test accuracy.

Overall test accuracy is defined as:

$$A = 1 - \frac{|t - r|}{t}$$

where A is the <u>overall accuracy</u> for a test, r is the result determined by using the camera for counting, and t is the ground truth, which is determined by counting pedestrians manually and verifying through recorded videos. In some cases, overcounts and undercounts balance each other resulting in a high overall accuracy. Overcounting is the situation where more pedestrians are counted than are actually present. Undercounting is the phenomenon of failing to increment the count by missing pedestrians. To understand the effectiveness of the approach, the counter-balancing of overcounts and undercounts should not be considered in determining the final accuracy. Hence, a second metric for accuracy is defined as

$$A = 1 - \frac{\Sigma o + \Sigma u}{t}$$

where o indicates errors caused by overcounts, u denotes errors derived from undercounts, and other notations are as defined in the first equation. The <u>accuracy</u> is equal to one minus the error, where the error equals the proportion of mistakes to the ground truth.

3.2 Results: State Averaging Approach

In an initial experiment at UMass, pedestrian counts were evaluated for a range of averaging constants, m, for pedestrians walking along a walkway. If m is defined as the averaging constant and N is the total number of detectors turning ON at a particular instant, the number of pedestrians at that instant is given by

$$\# Pedestrians = \frac{N}{m}$$

The corresponding accuracy values for different values of m are tabulated in Table 3.1 for seven video segments, each of six minutes.

20

Table 3.1: State averaging accuracy for each averaging parameter m. Values are listed as percentages of the true accurate count.

#Video	m = 10	m = 11	m = 12	m = 13
1	66%	83%	91%	100%
2	68%	81%	90%	100%
3	70%	81%	92%	100%
4	82%	93%	95%	89%
5	91%	100%	91%	84%
6	94%	96%	88%	81%
7	93%	96%	88%	81%

It can be concluded that *m=11* and *m=13* work best for the detector configurations. The <u>overall accuracy</u> and <u>accuracy</u> measurements, defined by on the previous page, were calculated over eight trials using the averaging approach with *m = 11*. In Table 3.2, the column labeled duration denotes the duration of a test with its unit as min:sec.

Table 3.2: Sweep table of accuracies according to two definitions of accuracy

Test	Duration	Ground truth	Result	Under counts	Over counts	Overall Accuracy	Accuracy
1	1:35	20	20	2	2	100%	80%
2	0:35	7	6	1	0	85%	85%
3	0:33	9	10	0	1	88%	88%
4	0:26	8	8	0	0	100%	100%
5	1:07	37	34	4	1	91%	86%
6	0:26	24	21	3	0	87%	87%
7	0:32	30	29	3	2	96%	83%
8	0:05	9	8	1	0	88%	88%

The effect of pedestrian flow rate on the accuracy of the state averaging algorithm was also examined. Flow rates greater than 50 persons/second can be considered a crowd, indicating occlusion caused by the overlap of pedestrians in the image. This overlap may potentially cause undercounts. Table 3.3 investigates this issue.

Table 3.3: Sweep table of accuracies versus pedestrian flow (persons/min)

Test	Duration	Flow	Ground truth	Result	Under counts	Over counts	Overall Accuracy	Accuracy
1	1:35	8	20	20	2	2	100%	80%
2	0:35	12	7	6	1	0	85%	85%
3	0:33	16	9	10	0	1	88%	88%
4	0:26	18	8	8	0	0	100%	100%
5	1:07	33	37	34	4	1	91%	86%
6	0:26	55	24	21	3	0	87%	87%
7	0:32	56	30	29	3	2	96%	83%
8	0:05	108	9	8	1	0	88%	88%

Results in Table 3.3 indicate that accuracy is generally unaffected by pedestrian flow rate. This consistent accuracy from the averaging approach establishes the robustness required for wide scale deployment. Detectors partially covered by shadows were ON despite the constant state of the background during the refresh interval. Objects must cover at least one-fourth of a detector region to cause an OFF-ON transition.

During experimentation it was found that pedestrians that are closer to the camera occupy less image area than pedestrians who are farther from the camera. Hence, detectors were configured in two columns with non-uniform spacing, similar to the spacing shown in Figure 3.2 for a single column. Hence, more detectors were placed in areas of higher density. The observed results for $m = 11$ are shown in Table 3.4.

Table 3.4: Sweep table of accuracies versus pedestrian flow for $m = 11$

Test	Duration	Ground truth	Result	Undercounts	Overcounts	Overall Accuracy	Accuracy
1	0:26	9	8	1	0	88%	88%
2	0:37	35	31	6	2	88%	77%
3	0:18	20	16	4	0	80%	80%
4	0:20	30	26	5	1	86%	80%
5	0:17	21	17	4	0	80%	80%
6	0:11	16	14	2	0	87%	87%

The two-column configuration of 15 detectors with uniform spacing generally gave the best accuracy values for the averaging approach. Undercounting was a more significant source of error. Shadows did not degrade accuracy under dense pedestrian traffic because of occlusion. However, under low traffic conditions, overcounts occurred for the shadows of pedestrians crossing the detector region.

Figure 3.2: Detector configuration with non-uniform spacing

3.3 Results: State Matrix Approach

This approach was formulated to address scenarios where sufficient detectors do not turn ON for averaging. In all conducted real-time trials, the average accuracy for this approach was found to be 40%, primarily due to undercounting. Hence, detailed analyses of the results were not performed and the approach was abandoned.

3.4 Results: Threshold Approach

The threshold approach was also not found to be robust for a range of locations, mounting heights and camera angles. Accuracies ranged from as low as 45% to as high as 99% for selected trials. The lack of consistency and robustness against irregular pedestrian traffic movements discourage its use in wide scale deployment. For these experiments, vertical detector groups consisted of N consecutive detectors. In some cases, adjacent groups overlapped by O detectors. A total of at least M detectors (the threshold) needed to be triggered out of the N consecutive detectors to indicate a positive detection.

It was found that a significant number of undercounts took place when $M \geq 0.75 \times N$ and the amount of detector overlap between adjacent groups of M detectors was $O \leq 1$. Alternatively, overcounts contributed to error when $M \leq 0.75 \times N$ or when overlap $O = 0.5 \times N$. Configurations with different numbers of detectors were tried. It was found that a configuration of 15 detectors each of size 9 x 2 pixels in a column gave the best performance with groups of detectors overlapping by $O = 0.25 \times N$ and when $M = 0.75 \times N$. It can also be concluded from experiments that uneven groups, for instance three groups with values of N of 6, 5, 6, gave better consistency in accuracy than evenly divided groups. This finding can be explained by the fact that pedestrians farther away from the camera occupy more space in the image when compared to pedestrians closer to the camera. The resultant accuracies from various detector configurations per column are shown in Table 3.5. Each test was performed over 6 minutes. The detector configuration was similar to the one shown in Figure 2.8.

Table 3.5: Sweep results from threshold approach

#detectors	N	M	overlap	Average flow rate (ped/min)	Accuracy
11	5	4	2	5.7	74%
13	5	4	1	25.2	80%
15	5	3	0	17.9	80%
15	5	4	0	17.9	80%
15	6,6,5	4,4,3	1	17.9	74%
15	6,5,6	4,3,4	1	17.9	70%
15	6	4	2	17.9	83%
15	6	4	3	17.9	55%
15	4	3	0	17.9	77%
15	4	3	1	17.9	62%

Detectors of dimensions ranging from 2 to 10 pixels were used to provide redundancy for the multiple detector M of N approach. Larger detectors (2 x 10 pixels) gave rise to overcounts. Highly dense detector configurations were very sensitive to the values of M and N and the amount of region overlap.

3.5 Effect of Background Refresh Rate

During counting, background refresh rates for the presence detectors were fixed to 20, 60, 90 and 600 seconds. Refresh rates of 60 seconds and higher did not affect count accuracy. The low refresh rate of 20 seconds led to random detector state transitions although accuracy was not degraded since the count was only updated when a minimum number of detectors were turned ON.

3.6 Bicyclist Detection and Counting

Experiments with different speed detector configurations were performed to evaluate the Solo Terra's ability to count bicyclists and differentiate them from motor vehicles. A main challenge of experimentation was to differentiate between a bicyclist and a motor vehicle which may be accidentally driven in a bicycle lane. In order to emulate real traffic scenarios with bicyclists and motor vehicles, experiments were conducted at a sidewalk and bicycle lane adjacent to North Pleasant Street near the University of Massachusetts, Amherst. The experimental setup is shown in Figure 3.3.

Figure 3.3: Experimental setup for bicyclist detection
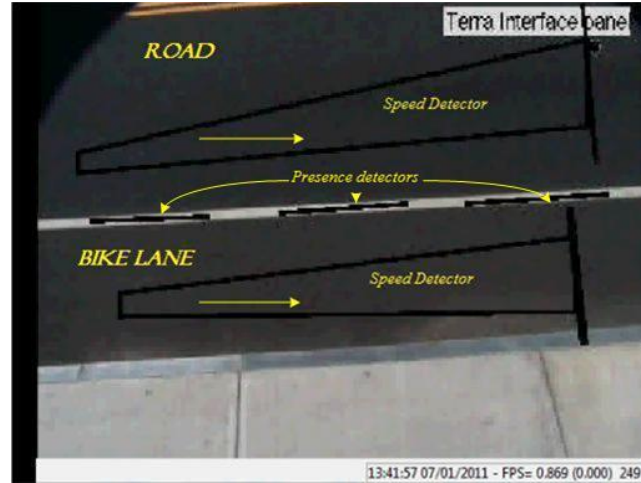
In an initial test, a configuration consisting of two speed detectors was configured onto the Solo Terra, with one detector covering the bicycle lane and the other detector over the adjacent traffic lane, as shown in Figure 3.3. In actual deployment, only one speed detector on the bicycle lane would be needed. For three different video feeds, the data collected by the speed detector in the bicycle lane is tabulated as shown in Table 3.6.

Table 3.6: Speed and length information for five bicyclists measured in a bicycle lane

Bicyclist	Speed (miles per hour)	Length (feet)
1	12	6.1
2	12	8.5
3	8	6.0
4	15	7.1
5	10	5.6

The average speed of a bicyclist was found to be 11.4 MPH and the average length was determined to be 6.4 feet, somewhat of an overestimate of the length of a typical bicycle. The speed and length measurements by the traffic lane speed detector indicate that some motor vehicles have a similar speed and length, making differentiation difficult. Thus, speed alone cannot effectively be used as the distinguishing feature to differentiate between bicyclists and motor vehicles. However, most motor vehicles recorded a length of more than 8 feet, with a few exceptions. The average measured length of a motor vehicle was found to be 12 feet, again somewhat of an overestimate. Thus, length can be used as a differentiating parameter. A simple thresholding algorithm was used with vehicles with lengths less than 8 feet being classified as bicycles and the rest as motor vehicles. With this approach, we achieved a detection accuracy of less than 70%. The faulty data values resulting in the limited current accuracy were a result of the speed detector configuration. To solve this problem, recalibration of the speed detectors was carried out. The speed detectors were calibrated with a downlane distance of 50 feet and a crosslane distance of 10 feet. The downlane is the area of the road parallel to the direction of motion and the crosslane is the area of road perpendicular to the direction of vehicle motion. Recalibration improved the accuracy of detection, giving consistent length results for bicyclists and motor vehicles. The detection results for bicyclist and motor vehicles after recalibration are shown in Table 3.7.

Table 3.7: Detection results for bicyclists and motor vehicles using Solo Terra speed detector zones

Bicyclists		Motor Vehicles	
Ground Truth	Count	Ground Truth	Count
9	9	27	23

A value of 100% accuracy in bicyclist detection was determined using the thresholding approach. For motor vehicles, there was an undercount of 4, giving an accuracy of 85.2%. In some cases, the motor vehicle length was recorded as shorter than the threshold leading to classification as a bicyclist. Since bicyclists can be independently counted without error, an erroneous bicyclist count can only occur due to a motor vehicle being mistakenly counted as a bicyclist. There was no instance when a bicyclist was erroneously counted as a motor vehicle. Hence, the bicyclist detection error rate was the same as the failed motor vehicle detection rate, i.e. 14.8%. In experiments where no motor vehicles entered the bicycle lane, a 100% accuracy of bicyclist detection was achieved.

Since the final objective of this project is to count pedestrians and bicyclists together, a single configuration was designed that can detect both classes simultaneously. The camera height and tilt angle were adjusted such that it captures both the sidewalk and the bicycle lane. The integrated configuration is as shown in Figure 3.4 below.

Figure 3.4: Integrated configuration for detecting pedestrians and bicyclists

Two columns of 15 count detectors each were placed on the sidewalk to count pedestrians. The spacing between adjacent detectors in a column had to be reduced, as the area covered by the sidewalk is relatively smaller than the case where separate configurations are used for pedestrians and bicyclists. Due to this reduction in spacing between detectors, each person triggers more detectors leading to a change in averaging factor of the state averaging algorithm. Experiments suggested that 14 detectors give the best accuracy for counting pedestrians. The overall accuracy of detection was found to be in the range of 85-90%, suggesting the absence of any deterioration in accuracy using the combined configuration as compared to a separate pedestrian configuration.

In order to detect bicyclists, the same speed detector configuration as described earlier is used. However, if a pedestrian is walking very close to the edge of the sidewalk and is aligned with the speed detector, there is a possibility of him/her triggering the detector. This action can result in the pedestrian being erroneously counted as a bicyclist, leading to bicyclist overcounts. Through experiments it has been found that reported pedestrian lengths are smaller than those of bicyclists. Thus, by using a minimum threshold value in the algorithm which is greater than the average pedestrian length, it is possible to ensure that a pedestrian is not erroneously counted as a bicyclist even if he/she triggers the detector. The accuracy of counting bicyclists was found to be 90% and the loss of accuracy was mainly due to overcounts caused by pedestrians erroneously triggering the bicyclist count. Such false triggering of the bicyclist count can occur in situations when a pedestrian stays in the detection zone for too long, erroneously registering his/her length as being longer than the length expected by the speed detector.

3.7 Results from Integrated System

3.7.1 Training for Histogram of Gradients Approach

Prior to experiments with combined state averaging and HoG image processing approaches, calibration was performed using a separate small camera and processing with the HoG approach described in Section 2.3. A Sony NSC-GC1 camera was used for vision-based HoG shape detection. The camera collects video in MPEG4 format with a frame size of 640 x 480 and a frame rate of 30 frames per second. The camera supports the streaming of 320 x 240 video frames using a 32-bit Windows operating system.

To reduce false detections and ensure real-time operation, only a section of each frame containing the sidewalk was scanned for pedestrian heads and shoulders. Overlapping or non-overlapping rectangular scanning regions were specified prior to the experiment. The first frame of streaming video was used to select the processing area in subsequent frames. The selected region coordinates were rounded off to nearest multiples of the window size and subsequently processed by the software. Figure 3.5 illustrates detections regions (blue rectangles) and identified pedestrians (green rectangles).

Figure 3.5: Scanning for omega shapes in user-selected frame regions

During experimentation, it was found that pedestrians cross a 10 pixel wide region in under a second. Hence, two seconds of activity signified by sixty frames were buffered to determine the background, as described in Section 2.3.2. It was determined through experiments that color and context information aid detection. A camera mounting height of 20 feet ensures that a pedestrian's head and shoulders fit into a 32 x 32 pixel sized window. The entry of a pedestrian into a window is signified by change in more than 250 of the 1024 pixels in the window (32 x 32). Hence, the HoG of a window in the frame is calculated if more than 250 pixels in the scanned window change values. This approach ensures the real-time operation of the HoG detection algorithm. As described in Section 2.3.4, a training data set was used to assist the classifier in identifying possible pedestrians. The block and cell size were fixed to 8 x 8 and 4 x 4 pixels respectively. The optimum HoG parameters for detecting the "Ω" shape are listed in Table 3.8.

Table 3.8: Optimum values of parameters for "Ω" detection

Parameter	Value
Window Size	32 x 32 pixels
Sliding distance for windows	8 x 8 pixels
Block Size	8 x 8 pixels
Cell Size	4 x 4 pixels
Number of bins in the histogram	8

The total processing time for a one-minute video with a processing rate of one frame per second is one minute with the implemented HoG software. A pedestrian detection accuracy of 80% was achieved over a set of six video sessions, each of duration two minutes. The benchmark videos were collected at walkways at the University of Massachusetts, Amherst. The percentage of time spent in each function as reported by the *gprof* software tool is reported in Table 3.9.

Table 3.9: Execution time reported by gprof for portions of the HoG algorithm

Function	% of time spent for execution
Gradient Calculation	51.26
Histogramming	45.13
Classification	3.56
Others	0.05

3.7.2 Results of integrating state averaging and histogram of gradients approaches

Preliminary experiments were carried out to evaluate the functionality of the integrated approach. Two image conditions were identified. One condition scans for omega shapes when more than a certain number of Solo Terra detectors are ON during a one second period. The second condition scans for omega shapes when more than a certain number of detectors remain ON for a pre-determined period. The Solo Terra was configured with two columns of 15 presence detectors. Five scenarios were considered for the integrated approach.

- A group of five people walking along a walkway
- A group of four people walking along a walkway
- A group of three people walking along a walkway
- Multiple groups of two people walking along a walkway

28

- A single person carrying a box.

The detector activation counts determined by the Solo Terra were dumped into a text file. It was found that the HoG approach can correct the Solo Terra count determined using state averaging when 4 or more people walk across the detector region in a single line as shown in Figure 3.6. In all other cases, the count determined by the state averaging approach was determined to be sufficient without correction. Accuracy results for the conducted experiment are tabulated in Table 3.10.

Table 3.10: Preliminary results for the integrated approach

Ground truth	Count from Solo Terra approach	Count from HoG approach only	Count from integrated approach
34	29	27	32

Figure 3.6: Scenario where count gets corrected by the HoG approach in the integrated system

The accuracy for the integrated approach is highly sensitive to the region demarcated for the omega shape search and the amount of window overlap. A slight variation of 6 pixels may affect the accuracy in the presence of dense pedestrian traffic. The processed area is divided into 32 x 32 windows and scanned for HoGs.

Figure 3.7: Scenarios which invoked omega detection algorithm but did not increment count

The omega detection approach generally performs poorly under occlusion and heavy pedestrian traffic. There were cases when the omega formed by the head of a person was not detected when the HoG approach was invoked for making a correction. In such cases, pedestrian counts obtained

from the state averaging algorithm cannot be improved. For example, the photo on the left in Figure 3.7 shows the occlusion of the shoulders of one of the pedestrians.

4.0 Implementation/Tech Transfer

In the following subsections, a series of recommendations for widespread deployment of the system are presented. These recommendations cover both the system software and deployment options for daily use of the system.

4.1 Software Enhancements

Specific software enhancements to improve the usability of the system could include:

- The current zone-based pedestrian and bicyclist counting approaches could be integrated into the camera itself. This action would allow for the replacement of the laptop with a much simpler computing device (e.g. $150 netbook) since the compute-intensive algorithms would be implemented in the camera. The netbook would still be needed to allow for the transfer of the final count value to a memory stick or via wireless communication.
- The software inside the Autoscope camera could be adjusted to prevent frequent image background updates and provide greater tolerance for occasional bursts of sunshine which have been shown to affect count accuracy. Also, the size and number of detection zones could be adapted to potentially support increased count accuracy.

4.2 Widespread Deployment Options

Based on our experiences using the camera, we can make the following recommendations regarding widespread deployment of the system. We envision three scenarios in which the system could be deployed to collect pedestrian and bicyclist count information on a daily basis. We expect that the system could be taken from a local transportation facility each morning and set up on the side of an urban sidewalk. Pedestrian and bicyclist counts could then be collected at the end of the day and the system could then be returned to the facility. The following specific steps could be used to accomplish this task:

1. The detection and counting equipment (camera, support structure, interface board, and PC) on a trailer are attached to a vehicle.
2. After reaching the test location, the equipment is assembled, configured, and set up on the roadside.
3. The sidewalk sight line camera is adjusted and the software algorithms on the camera and attached PC are started.
4. The count is started and information collection is performed (count, collection time, density, etc) on the attached PC.
5. After the period of the experiment (e.g. 1 to 8 hours) the count is downloaded from the PC to a memory stick. It may also be possible to transmit the information wirelessly from the PC attached to the camera to an alternate PC.

6. The equipment is disassembled and transported away. Other than the count and collection time, no further information is stored on the PC.

This first scenario was demonstrated during an experiment performed in Boston on August 30, 2011. A second scenario could allow the camera and associated PC to be mounted for an extended period of time on a building or traffic sign post. This action would preclude the need for daily transportation and setup of the equipment at the experiment site. The PC could be located in a nearby traffic control cabinet. A limitation of this approach is the need for AC power. A third, less likely scenario for deployment could involve the retasking of an existing traffic camera which has already been deployed for use in vehicle traffic control. The PC could be located in an adjacent traffic control cabinet.

4.3 Deployment Location Options

The system has been specifically developed to operate on urban sidewalks. It has been demonstrated that accurate counts can be obtained for a variety pedestrian traffic densities, including dense traffic of over 100 pedestrians per minute. Given this information, we believe that the system can be effectively deployed on an urban roadside both near intersections and in the middle of city blocks. Additionally, the system could be effectively deployed on a shared use path for either pedestrian or bicyclist traffic. It would be difficult to detect and count both types of traffic simultaneously on shared use paths since both types of traffic would share the same roadway.

4.4 Other Issues

To date, the system has not been tested in inclement weather (e.g. snow, rain) or at night. Additional testing and possible algorithm adjustment would be necessary for deployment under these circumstances. It may be also be possible to eventually replace the expensive Autoscope Solo Terra camera with a lower cost alternative. This approach would require the independent development of the zone-based detection capability on images transferred to a PC. Although this effort would likely require significant engineering, the cost of the camera system could be reduced from about $4,000 for the current system to less than $1,000.

4.5 Next Steps

Although the algorithms used in our experiments have been shown to be quite accurate, a series of enhancements is envisioned for future systems:

- Currently, the algorithms can accurately detect up to three pedestrians walking through detection zones side-by-side. Wider sidewalks with more pedestrians could be investigated in the future.
- The integrated HoG and state averaging approach is still in a fairly preliminary state. More advanced experimentation using a broader set of camera angles could be considered.

- The use of the system on a shared use path would likely require additional tuning since the current system assumes a segregation of the areas for pedestrian and bicyclist traffic. It may be possible to overlap the presence detectors used for pedestrian detectors with the speed detectors used for bicyclist counting.

Additional algorithms could also be considered to validate counts over a longer time span (e.g. 8 hours or more).

5.0 Conclusions

This project has implemented an automated system to count pedestrians on a sidewalk and bicyclists in an adjacent bicycle lane. The main objective of the work is to aid urban transportation planning. Two camera-based approaches were integrated for the detection and counting of pedestrians. The first approach uses an Autoscope Solo Terra device, a widely-deployed traffic camera. This approach uses presence detection zones to identify pedestrians passing through specific regions of an image. The pedestrian count is incremented based on the number of zone detectors that are triggered. The second, complementary approach uses vision-based shape detection. This approach detects pedestrians based on images of their head and shoulders. The Autoscope Solo Terra approach was found to provide over 85% pedestrian counting accuracy in many experiments. The vision-based shape detection approach allowed for improved accuracy for situations with many pedestrians (e.g. 4) walking abreast. A system for bicyclist detection and counting was also implemented using the Autoscope Solo Terra camera. This approach uses speed detection zones to measure a bicyclist's speed and length. If both bicyclists and motor vehicles are detected in a bicycle lane, an accuracy of 85% is achieved. If only bicyclists are detected in the lane, nearly 100% accuracy is obtained. A robust mounting platform based on a trailer was designed and implemented for the system along with a detailed user's manual. The system is available for immediate deployment by MassDOT. In the future, a more robust software system for both pedestrian and bicyclist counting will be developed and refined. Additional enhancements for the counting algorithms are planned.

As a result of this work, it is recommended that a pilot project be established that allows for the extensive collection of bicyclist and pedestrian data in a variety of real world urban roadway environments. Given the immediate need for this data and the availability of the functional prototype, the collection of this data can have significant short and long term benefits for urban transportation planning.

6.0 Appendix – Instruction Manual

6.1 Assembling the camera support structure

1. Arrive at the test site and unhook the trailer. Install the trailer's five stands against ground. Get all the components (camera, mast, Ethernet cable, laptop power cord, tool bag etc.) from the storage cases. Place the laptop in the black laptop case (the one sitting in the horizontal position).

2. Open the black interface panel case (the one standing vertical) and pull out the two cables – the black camera cable, and the yellow interface panel power cord, through the hole at the bottom of the case.

3. Make sure that the switch (marked RED) near to the black camera cable is in the ON position. If it is not, then the camera will not be powered.

4. To assemble the camera on top of mast, place the nuts between the camera and the vertical plates of the camera mount as shown below. Tighten the nut using the wrench so that the camera is stable, though it should be able to tilt up and down with some resistance. Tilt the camera so that it approximately makes an angle of 30 degrees with the pole. Keep the mast retracted while assembling.

5. Remove the protective lens cover from the camera.

6. Attach the camera cable from the interface panel to the camera as shown in the picture. Markings on the cable plug and the camera socket can be matched to fit the plug correctly. Flip down the latch on the cable, to lock the cable and the camera together.

7. Place the mast on the mount structure located on left-hand side of the trailer.

8. Secure the higher end of the mast by fixing the bracket around it. While affixing the bracket tight, make sure that the camera is facing the road, perpendicular to the edge of the trailer.

9. Once the mast is secured, draw out the second layer of the mast upwards to the point it is locked with the red button. The first layer is not chosen to make sure that the pole does not sway with wind once the mast is drawn out at a higher level. Using the second layer improves the thickness of the mast, and thus its stability.
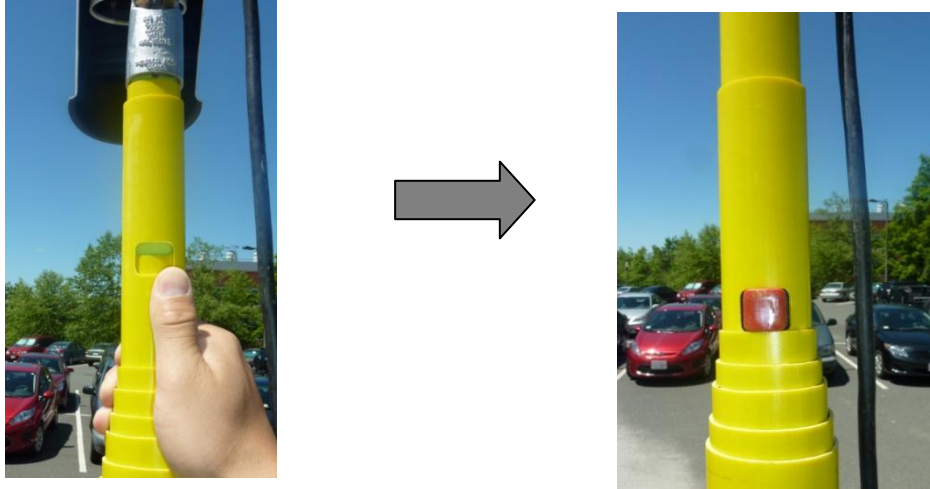
Note: To avoid injury, it is advisable to use a ladder to draw out the mast as both hands would be occupied in this exercise.

10. The resulting structure should look like as shown in the picture below.

11. For powering the system, connect the inverter and the batteries present in the yellow storage case. The red clipper must be attached to any battery terminal with a red wire connected to it. Similarly, the black clipper must be attached to any terminal with a black wire connected to it.
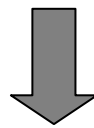
12. Plug the power cables of the interface panel and the laptop into the two inverter sockets through the side hole of the battery cabin. Plug the other end of the laptop power cable into the laptop through the bottom hole of the laptop case. Turn on the inverter using the ON-OFF switch. A green light indicates that the inverter is generating AC power.

13. Use the Ethernet cable to connect the interface panel and the laptop. One end of the cable is connected to the Ethernet port of the Autoscope interface panel, while the other end is connected to the Ethernet port of the laptop. Pass the cable through the bottom hole of the interface case and through the side hole in the laptop case.

14. Close and secure the interface panel case and the battery case with the provided locks.

15. The system assembly is now complete and is ready for use.

6.2 Software setup

6.2.1. Setting up the camera software

1. Boot up the system and log in to Windows using the MassDOT user account. The password is: **massdot**. The desktop screen should look like as shown in Figure 6.1.

Figure 6.1: Initial desktop screen

2. On the desktop, right click on the **Autoscope Network Browser v9.6.0_GLOBAL_2010-June-2** (Autoscope camera software) icon and select **Run as administrator.** Select **Yes** on the following dialog box.

3. Once the application starts, select the **Learn** option on the **Learn Network** popup box. This allows the camera software to search for any Autoscope cameras that are connected to the computer. This is shown in Figure 6.2.

Figure 6.1: Learn network
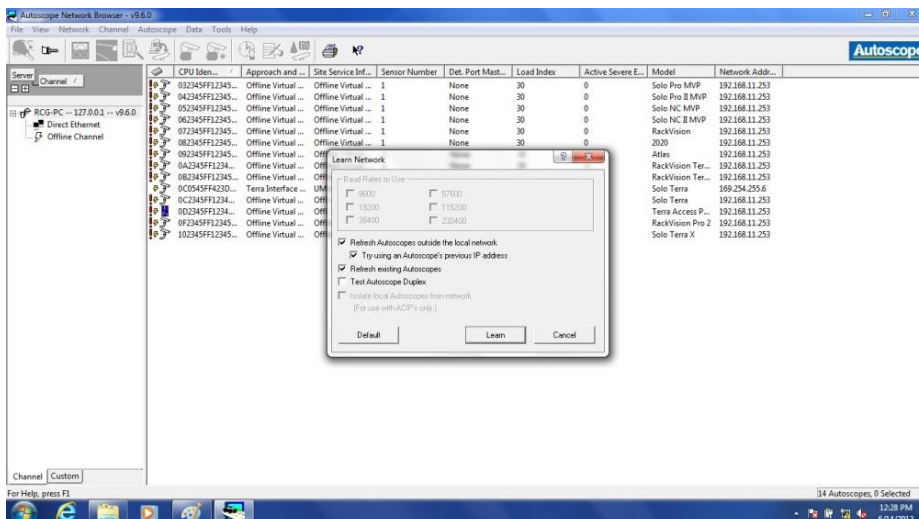
4. If the camera is connected properly, the software should find it as shown in Figure 6.3. Sometimes, if the camera is not found, close the network browser and restart again. If it still does not find the camera, select **Direct Ethernet** from the left-hand side pane and select the camera name in the right-hand side panel. Now click the **Channel** option from the menu bar at the top and select the **Learn** option. This starts the learning process again in order to find the camera.

Figure 6.2: Autoscope software searching and finding the connected camera
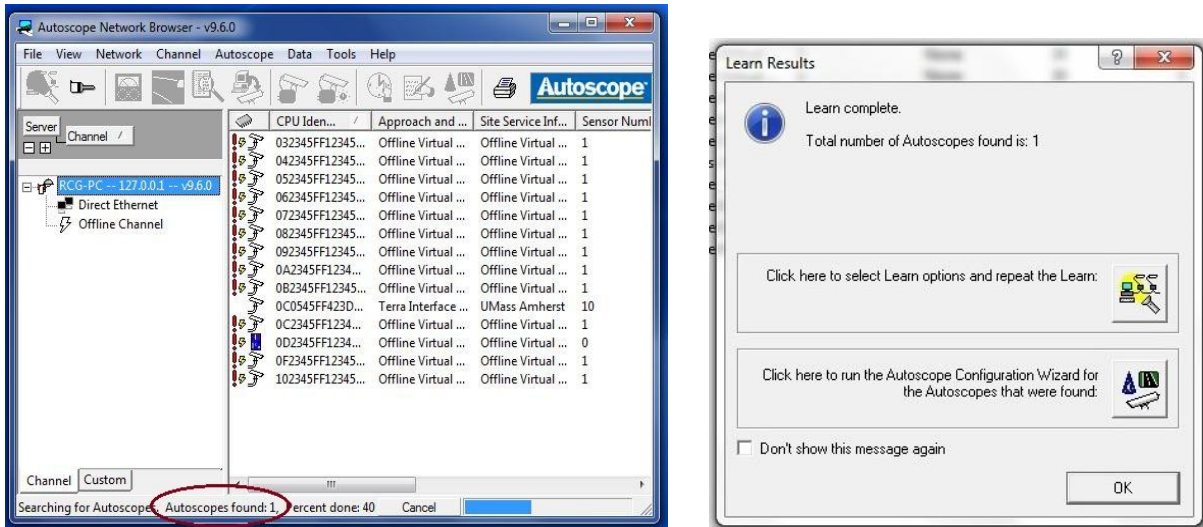
5. Select **Direct Ethernet** from the left-hand side panel and then select the only option on the right-hand side (which shows the Autoscope camera information), as highlighted in Figure 6.4. Also note the menu and the toolbar as shown in Figure 6.4.

**Figure 6.3: Selecting the camera on the direct Ethernet channel**
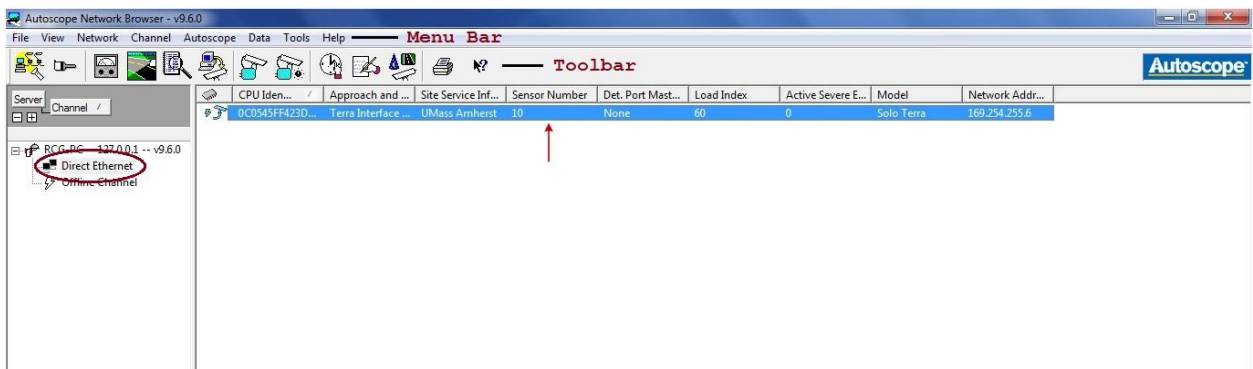
6. In order to make sure that the camera is capturing the detection zone properly, view the live video feed of the detection zone by clicking the **View Video** icon on the toolbar as shown in Figure 6.5. This starts the **Autoscope Video Player**. Pop-up the window from the taskbar located at the bottom of the screen by clicking on its icon.

Figure 6.5: View video icon can be pressed to start video
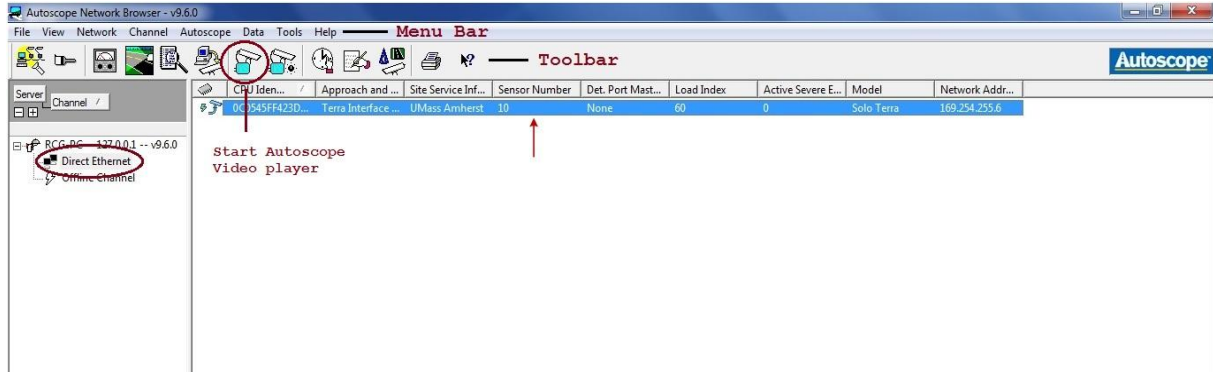
7. To start playing the video, click the green play button on the top left corner as shown in Figure 6.6, select **Continue detecting while streaming video** option in the following popup dialog box and click **OK**.

**Figure 6.6: Playing the video in Autoscope video player**

44
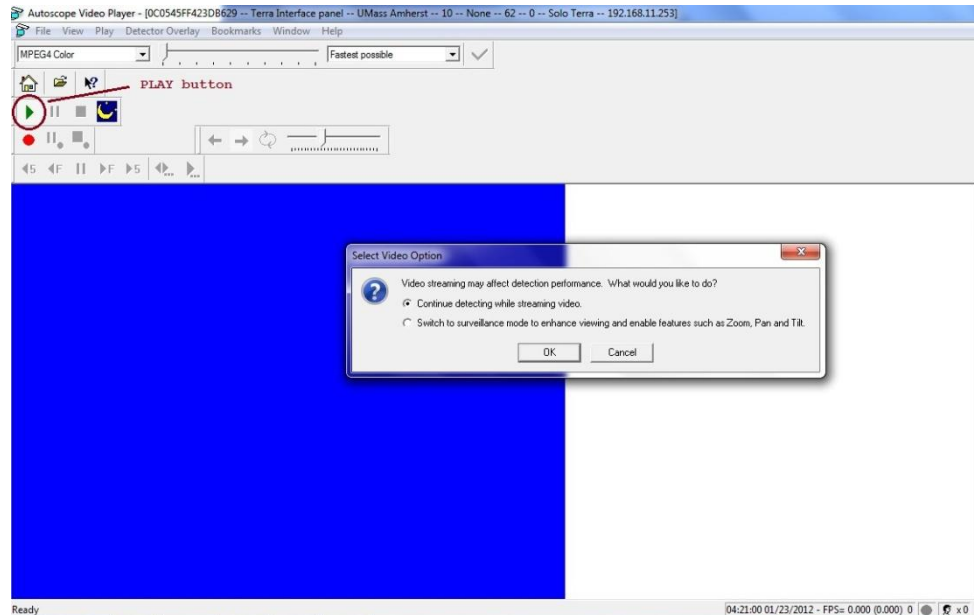
8. The video shows the current detector configuration of the camera, superimposed on the image of the detection zone as shown in Figure 6.7. The count detectors are used to count pedestrians, whereas the speed detector is used for counting bikes.

Figure 6.7: Autoscope video output

9. Adjust the camera angle to make sure that the count detectors fall on the pedestrian path and the speed detector falls on the bike path as shown in Figure 6.7.

10. Minimize the Autoscope video player window and go back to the Autoscope Network browser window.

11. To set-up the data collector, select **Direct Ethernet** in the left window panel and select the camera information in the right panel (the only option). Then select the **Data** option from the menu in the network browser, and click on **Data collector** from the drop down list.

12. In the **Add Poll** box that will follow, there are three (3) vertical panels named as **Detector Types, Detectors, and Fields**. In the **Detector Types** panel, select the **Count Detectors** and **Speed Detectors** one after another by pressing down the **Ctrl** or **Shift** key. Click on the **Add Poll** button as shown in Figure 6.8 and close the dialog box.

Figure 6.8: Adding polling data – Select count and speed detectors
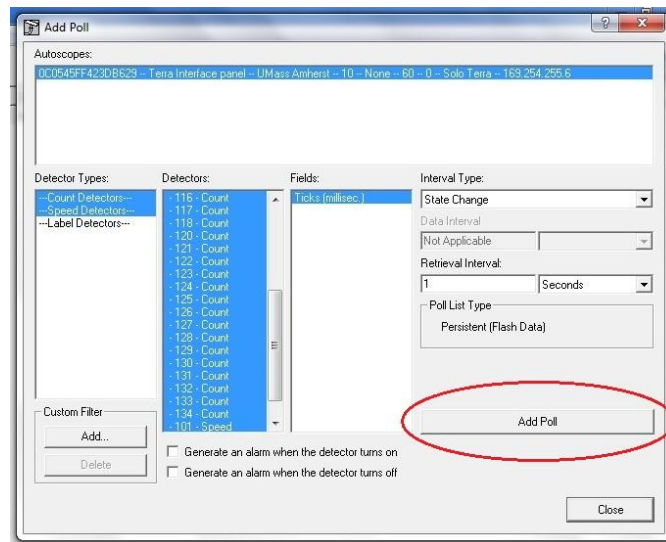
13. Start polling the data by clicking the **Start Polling** button circled in Figure 6.9. Wait for about 20 seconds for data collection process to start.

Figure 6.9: Start data polling – Autoscope Data Collector
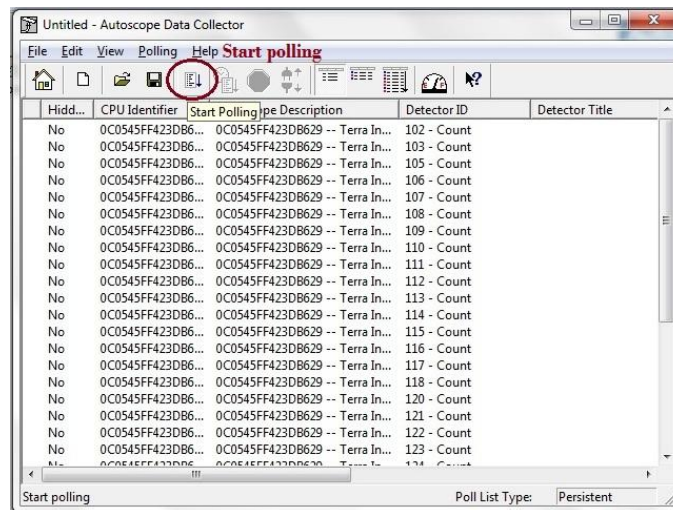
14. The camera software is now ready for collecting data and streaming video. Minimize all the open windows and return to the desktop.

6.2.2. Using the counting software

1. Navigate to the desktop and start the counting software by double-clicking the **Pedbike-Sunshine.exe or PedBike.exe** icon, depending on whether the weather condition is sunny or not.

2. From the **Count Option** menu, make a selection from the drop-down list. The option includes counting pedestrians and bikes, only pedestrians, and only bikes.

3. Press the **RESET** button to reset the system. The software **must** be reset in the beginning every time the application is started.

4. Press the **START** button to start counting. **RESET** the software every time the count option is changed.

5. Once the start button is pressed, hourly counts for both pedestrians and bikes are stored in a text file. The text file is named as **"log_(Date)_(Number)"** and is saved in the *Hourly Count Logs* folder on the Desktop. For e.g. for the date 17th July 2012, the log file would be named as *log_20120717_0*. Within the day, if the Autoscope software is closed and restarted again, the log file will be named as *log_20120717_1* and so on. A sample log file is shown in Figure 6.10.

Figure 6.10: Text file showing hourly counts

```
5:00 to 6:00 hours     Pedestrians = 6      Bikes = 5
6:00 to 7:00 hours     Pedestrians = 24     Bikes = 4
7:00 to 8:00 hours     Pedestrians = 54     Bikes = 0
8:00 to 9:00 hours     Pedestrians = 12     Bikes = 1
```

For more information on the counting software, please refer to section 6.4.

6.2.3. After-Use instructions

1. The counting software can be directly closed after the experiment.

2. The **Autoscope Network Browser** and the **Autoscope Video Player** can be closed normally like any other application by clicking the close sign button situated at the top right-hand corner of the window.

3. For closing the **Autoscope Data Collector**, first click on the **RED** stop button in the toolbar of the data collector window to stop the data collection process, as shown in Figure **6.11**. Say **Yes** to the following popup warning. Now close the data collector window by pressing the cross (x) sign on the top right hand corner like any other application. Say **No** to the following

popup dialog box. **Never close the Autoscope Data collector directly without stopping the process.**

**Figure 6.11: Closing the Autoscope data collector**
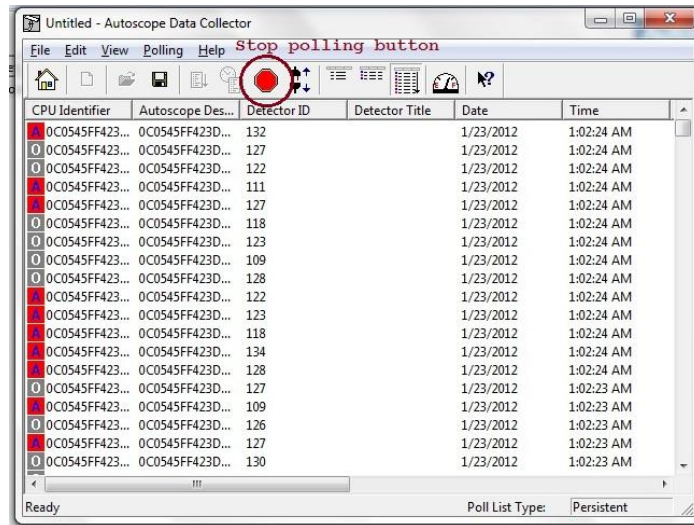
4. In case you happen to close the window directly, without stopping the process, open data collector, start the data collection process, wait for about 20 seconds for data collection to start, stop the process using the **RED** stop button, close the window and restart the data collection process again, starting with step 11 as mentioned in section A of the manual.

6.3 Disassembling the camera support structure

1. Close all software applications and turn off the laptop.

2. Open battery cabin and shut off the inverter using the ON/OFF switch. Unplug both the power cords.
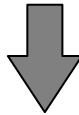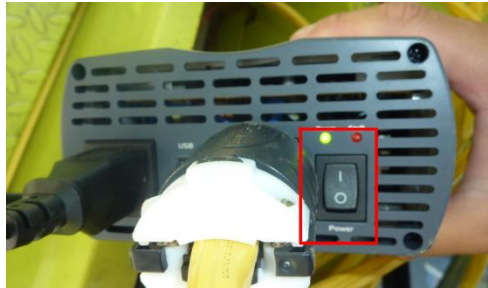
3. Disconnect the inverter from the battery. The inverter can be placed either in the separate storage case or can be left in the battery cabin.
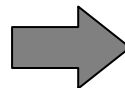
4. Unplug the Ethernet cable and the laptop power cord, and store them in the storage case.

5. Retract the mast and uninstall its upper mount bracket to get the mast and the camera off the trailer.

6. Disconnect the camera cable, unscrew the camera from the mast and store it in the storage case.

7. Retract the camera cable and the interface panel power cord into the interface panel case.

8. Place the storage case and the mast into the transportation vehicle.

9. Lock all cases and the battery cabin to fully secure the system.

6.4 More about the counting software

1. There are two versions of the counting software that are made available – **Pedbike-Sunshine** and **Pedbike**. As the name suggests, the former software is fine tuned to perform better in sunny conditions by taking the shadows into consideration, while the latter version is expected to work better on a non-sunny day. The user interface of the pedestrian and bike counting software is shown in Figure 6.12.

Figure 6.12: Designed pedestrian and bike counting software

2. The **START** button is used to start the counting process, when the software is started in the beginning. Once the **START** button is pressed, the software continuously keeps counting, and displays the pedestrian and bike count value in real time. The option to stop counting is not available - though the count can be reset to zero at any time using the **RESET** button.

3. Three (3) count options have been made available to the user – **Pedestrian only, Bikes only, and Pedestrian and Bikes**.

4. The counting option can be changed at any time and any number of times. Note that since the software is constantly updating the counts without any breaks, changing the count option does not automatically reset the respective counts to zero (0). It is the user's responsibility to manually reset the count using the **RESET** button, when switching between different options.

5. The user should make sure that there are no pedestrians or bicyclists passing by in between the duration, when the **RESET** button is pressed for the first time the software is launched, and pressing the **START** button. If you are unsure if any pedestrians or bikes have passed the detection zone, it is always a good practice to **RESET** the software again.

6.5 Modifying the camera detector configuration

The designed Autoscope Solo Terra system uses count detectors for counting pedestrians and speed detectors for counting bikes. These detectors can be configured manually in the detection field using an Autoscope provided software utility called as the **Detector editor**. The detector configuration is stored in file that can be opened and edited using the detector editor. Once a configuration is finalized, it can be send to the camera. The camera retains this configuration until a new configuration is reinstalled.

Currently, three different detector configurations are made available for detecting both pedestrians and bikes (configuration contains both count and speed detectors), only pedestrians (configuration contains only count detectors) and only bikes (configuration contains only speed detectors) respectively. The corresponding configuration files are located on the desktop and are named as **Ped+Bike.sdc, Ped_only.sdc** and **Bike_only.sdc** respectively. The current configuration installed on the camera has both types of detectors present, and hence capable of counting both pedestrians and bikes. However, if the need arises, this detector configuration can be modified or a different configuration can be installed using the steps detailed below.

1. Open the Autoscope network browser window and click the detector editor icon as shown in Figure 6.13.

**Figure 6.13: Opening detector editor in Autoscope network browser**
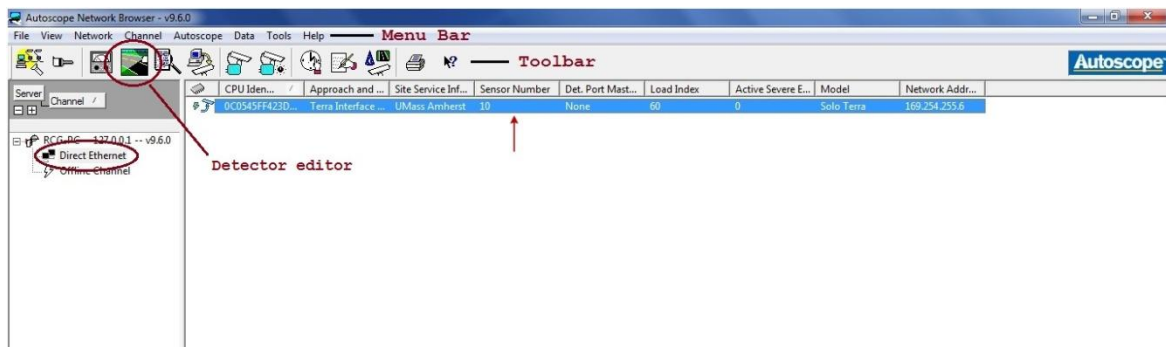
2. The detector editor window is as shown in Figure 6.14. The **Send File** button sends the configuration open in the editor to the camera. The **Get File** button gets the configuration that is currently residing on the camera. The red rectangles represent the count detectors that are placed in the current configuration.
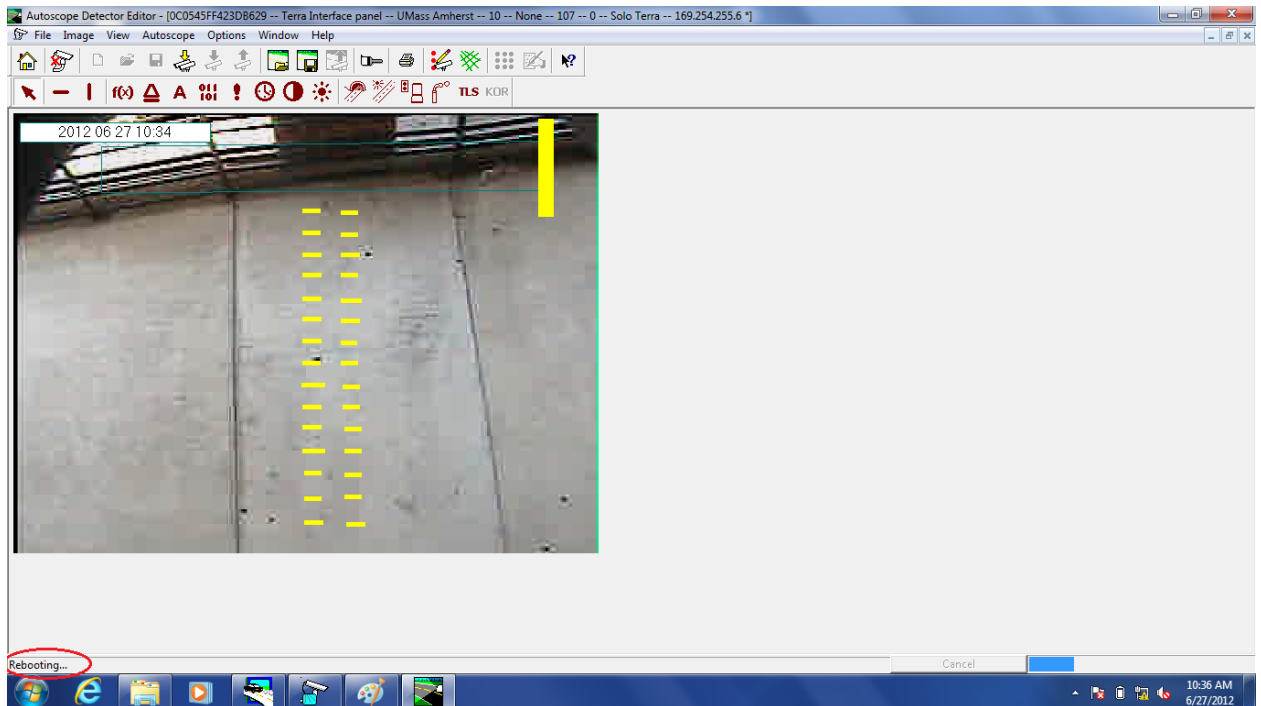
Figure 6.14: Detector editor window
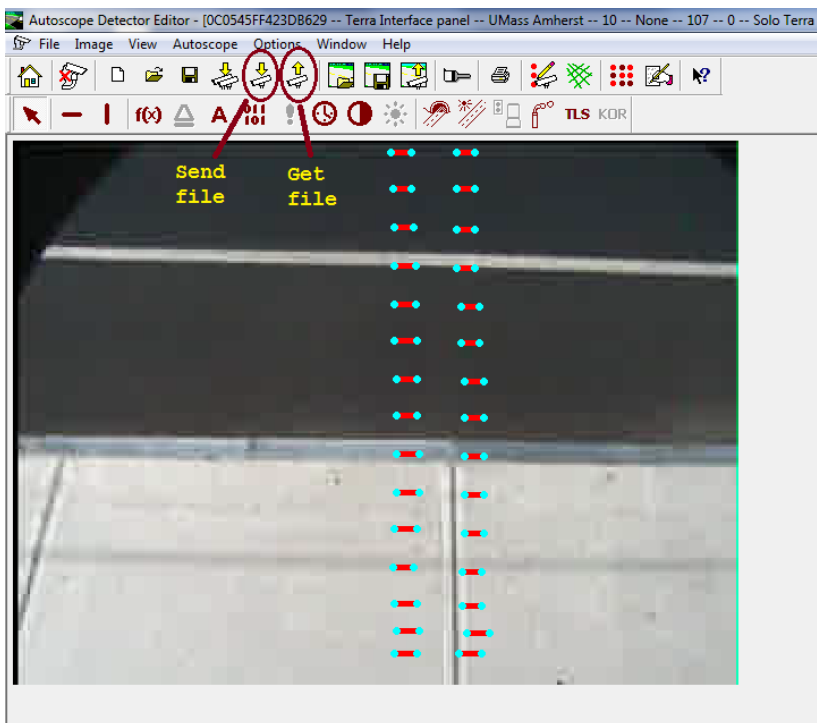
3. To open a configuration, click on the **File** option in the menu bar and click **Open.** Select the detector configuration and click **Open** as shown in Figure 6.15.

Figure 6.15: Opening configuration file
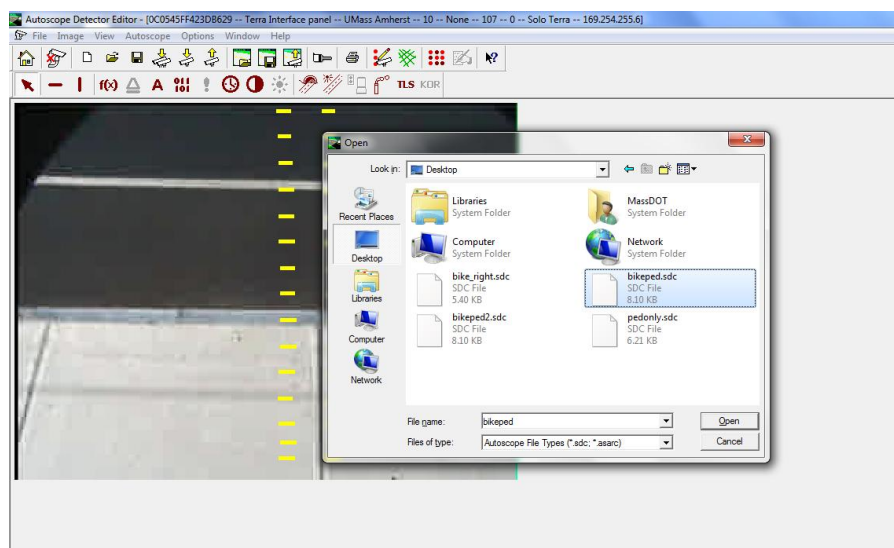
4. The detector configuration can be edited with the help of a mouse, e.g. changing the location of the speed detector to match the orientation with the bike lane, moving count detectors to cover pedestrian path etc.

5. After the editing is complete, click the **Send file** button to install the detector configuration on the camera. Once the button is pressed, the camera reboots to install the configuration as shown in Figure 6.16. After the reboot is complete, the camera holds the new detector configuration.

Figure 6.16: Installing detector configuration and camera reboot

6. Close the detector editor window.

7.0 References

1. U.S. Department of Transportation Federal Highway Administration, "PEDSAFE Crash Statistics, Pedestrian Safety Guide and Countermeasure Selection System", http://www.walkinginfo.org/pedsafe/crashstats.cfm, (Oct. 2011)

2. Minnesota Department of Transportation, "Analysis of Practical Methods for Counting Bicycles and Pedestrians," Technical Summary (Jun. 2010) 2 pp.

3. Michelat, T., Hueber, N., Raymond, P., Pichler, A., Schaal, P., and Dugaret, B., "Automatic Pedestrian Detection and Counting Applied to Urban Planning," *International Joint Conference on Ambient Intelligence*, (Nov. 2010) pp. 285-289.

4. Zhang, J., Tan, B., Sha, F., and He L., "Predicting Pedestrian Counts in Crowded Scenes With Rich and High-Dimensional Features", *IEEE Transactions on Intelligent Transportation Systems*, Vol. 12, No. 4, (Dec. 2011). pp 1037-1046.

5. U.S. Department of Transportation Bureau of Transportation Statistics, "Bicycle and Pedestrian Data: Sources, Needs, and Gaps," BTS00-02, Washington, D.C., (2000) 80 pp.

6. Padua, F., Campos, M., and Carceroni, R., "Real-Time Pedestrian Counting Based on Computer Vision", *Brazilian Conference on Artificial Intelligence*, (Sept. 2003) pp. 1-6.

7. Dalal, N., and Triggs, B., "Histograms of Oriented Gradients for Human Detection," *IEEE Computer Society Conference on Computer Vision and Pattern Recognition*, (2005) pp. 886-893.

8. Nanda, H. and Davis, L., "Probabilistic Template Based Pedestrian Detection in Infrared Videos," *IEEE Intelligent Vehicles Symposium*, (June 2002) 11 pp.

9. Fang, Y., Yamada, K., Ninomiya, Y., Horn, B., and Masaki, I., "A Shape-Independent-Method for Pedestrian Detection with Far Infrared-images," *IEEE Transactions on Vehicular Technology*, Vol. 53, No. 6, (Nov. 2004) pp. 1679-1697.

10. Noyce, D., Gajendran, A., and Dharmaraju, R., "Development of a Bicycle and Pedestrian Detection and Classification Algorithm for Active-Infrared Overhead Vehicle Imaging Sensors," *Annual Meeting of the Transportation Research Board*, Proceedings, Vol. 1982, No. 1 (2006) pp. 202-209.

11. Schwiezer, T., "Methods for Counting Pedestrians," *International Conference on Walking in the 21st Century*, (Sept. 2005) 11 pp.

12. Beezer, E., "Pedestrian Traffic Counting System," United States Patent 5946368, (1999)

13. Heikkila, J. and Silven, O., "A Real-Time System for Monitoring of Cyclists and Pedestrians," *IEEE Workshop on Visual Surveillance*, (Jun 1999) pp. 246-252.

14. Somasundaram, G., Morellas, V., and Papanikolopoulos, N., "Counting Pedestrians and Bicycles in Traffic Scenes," *IEEE Conference on Intelligent Transportation Systems*, (Oct. 2009) pp. 1-6.

15. Washington State Department of Transportation, "Washington State Bicycle and Pedestrian Documentation Project," http://www.wsdot.wa.gov/bike/Count.htm (2011).

16. Goebel, B., "MTA Begins Its First Automated Count of Cyclists," *SF.StreetBlogs.org*, (2009).

17. Econolite Corporation, "Autoscope Solo Terra Data Sheet," (2011) 2 pp.

18. Zhao, T. and Nevatia, R., "Bayesian Human Segmentation in Crowded Situations," *IEEE Computer Society Conference on Computer Vision and Pattern Recognition*, (Jun. 2003) pp. 459–466.

19. Burghes, J., "A Tutorial on Support Vector Machines for Pattern Recognition," *Data Mining and Knowledge Discovery*, No. 2 (1998) pp. 121-167

20. Schofield, C. and McFarlane, N., "Segmentation and Tracking of Piglets in Images," *Machine Vision and Applications*, Vol. 8 (1995) pp. 187-193.

21. Broggi, A., Bertozzi M., Fascioli A., and Sechi, M., "Shape-Based Pedestrian Detection," *IEEE Intelligent Vehicles Symposium*, (2000), pp. 215-220.

22. INRIA Person Dataset, http://pascal.inrialpes.fr/data/human/, (Oct. 2011)

23. OpenCV web site, http://opencv.willowgarage.com/wiki/, (Oct. 2011).